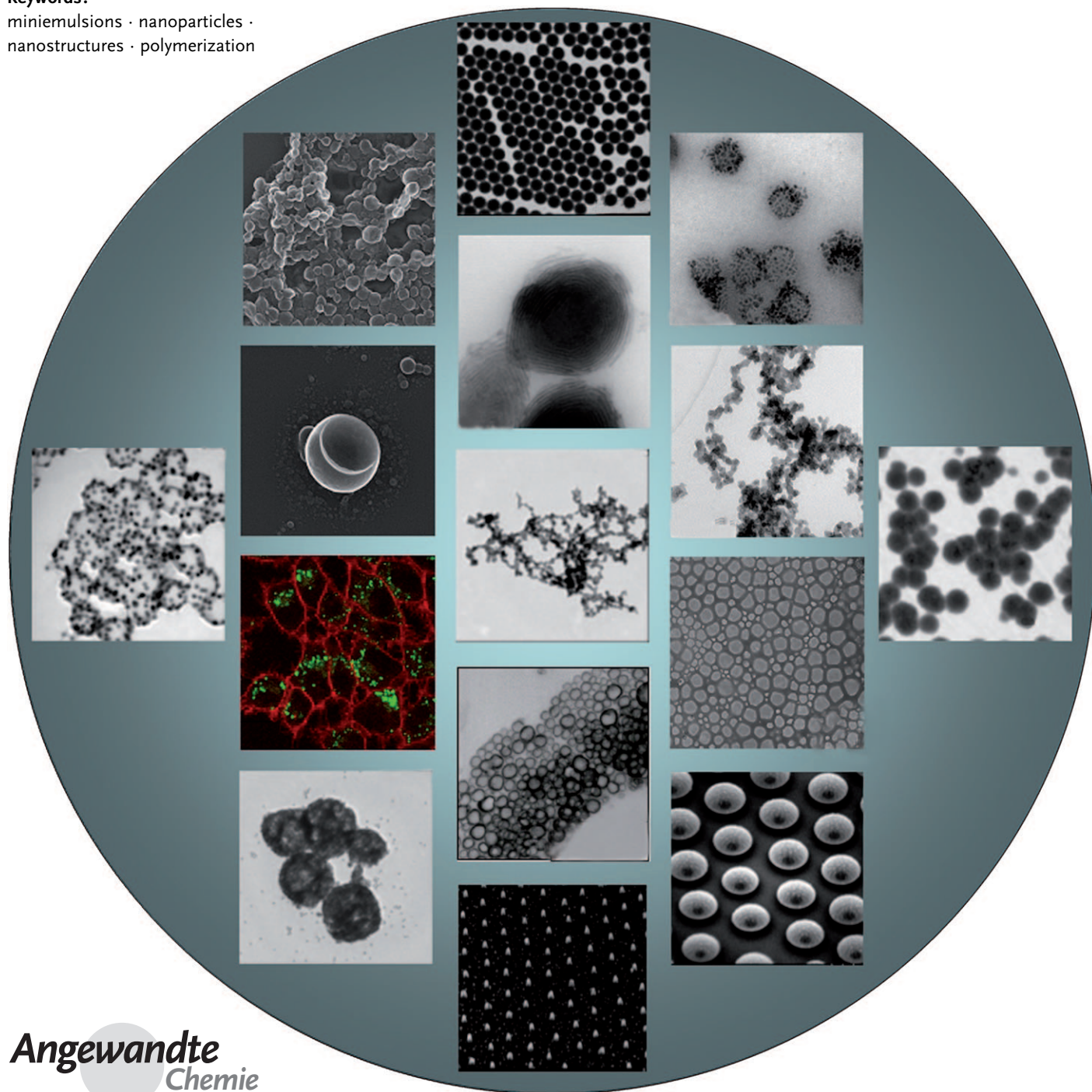


# Miniemulsion Polymerization and the Structure of Polymer and Hybrid Nanoparticles\*\*

Katharina Landfester\*

**Keywords:**

miniemulsions · nanoparticles ·  
nanostructures · polymerization



**T**he miniemulsion process allows the formation of complex structured polymeric nanoparticles and the encapsulation of a solid or liquid, an inorganic or organic, or a hydrophobic or hydrophilic material into a polymer shell. Many different materials, ranging from organic and inorganic pigments, magnetite, or other solid nanoparticles, to hydrophobic and hydrophilic liquids, such as fragrances, drugs, or photoinitiators, can be encapsulated. Functionalization of the nanoparticles can also be easily obtained. Compared to polymerization processes in organic solvents, polymerization to obtain polymeric nanoparticles can be performed in environmentally friendly solvents, usually water.

## 1. Introduction

The formation of structured polymeric nanoparticles and the encapsulation of a solid or liquid, an inorganic or organic, or a hydrophobic or hydrophilic material into a polymer shell is of great importance for many applications. Many different materials, such as organic and inorganic pigments, magnetite, or other solid nanoparticles for functional coating and other applications, can be encapsulated in a polymer shell. Compared to polymerization processes in organic solvents, polymerization to obtain polymeric nanoparticles can be performed in environmentally friendly solvents, such as water.

There are several heterophase processes that allow the formation of nanoparticles in water: the most well-known method is the emulsion polymerization technique, which is used in many industrial applications. However, this technique is mainly used for radical polymerization, and is not well-suited to the encapsulation of preformed polymeric or inorganic materials. The miniemulsion polymerization process is a very versatile technique for the formation of a broad range of polymers and structured materials in confined geometries.

In general, miniemulsions consist of small, stable, and narrowly distributed droplets in a continuous phase. The system is obtained by high shear; for example, by ultrasoni-

cation or high-pressure homogenizers. The high stability of the droplets is ensured by the combination of the amphiphilic component, the surfactant, and the co-stabilizer, which is soluble and homogeneously distributed in the droplet phase; the co-stabilizer has a lower solubility in the continuous phase than the rest of the droplet phase and therefore builds up an osmotic pressure in the droplets (it is therefore also called an osmotic pressure agent) counteracting the Laplace pressure. Such small droplets can then act as nanocontainers in which reactions can take place, either inside the droplets or at the interface of the droplets, resulting in most cases in the formation of nanoparticles. The miniemulsion process is shown in Figure 1; this review will highlight the wide variety of structures that can be formed and obtained by the miniemulsion process.

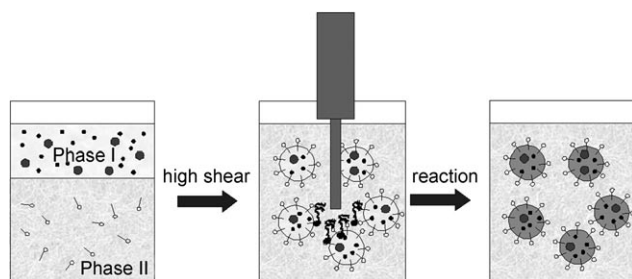


**Figure 1.** Principle of the miniemulsion process. Two immiscible phases are subjected to high shear, resulting in small, homogeneous, and narrowly distributed nanodroplets. Inside the droplet phase, an osmotic pressure agent and possible agents for further encapsulation are included. In a subsequent reaction process, ideally no change of the droplets is observed.

## From the Contents

1. Introduction	4489
2. Particle Formation	4490
3. Encapsulation of Soluble and Insoluble Materials	4491
4. Encapsulation of Liquids	4493
5. Phase Separation of Polymers inside Particles	4496
6. Functionalization of Nanoparticles and Nanocapsules	4499
7. Release from Nanocapsules	4499
8. Structure Formation of Inorganic Nanoparticles	4500
9. Crystallization in Nanoparticles	4502
10. Structuring with Nanoparticles	4503
11. Conclusion	4504

[\*] Prof. Dr. K. Landfester  
Max-Planck-Institut für Polymerforschung  
Ackermannweg 10, 55128 Mainz (Germany)  
Fax: (+49) 6131-379-370  
E-mail: landfester@mpip-mainz.mpg.de  
Homepage: <http://www.mpip-mainz.mpg.de>

[\*\*] Published on the occasion of the 25th anniversary of the Max Planck Institute for Polymer Research, Mainz.

## 2. Particle Formation

### 2.1. Polymerization in Miniemulsions

Polymerization in miniemulsions is possible over a very broad range. There is no doubt that radical polymerization can be performed with many different monomers (e.g. styrene, acrylates, methacrylates, fluoroacrylates, acrylamides). Copolymerizations between two hydrophobic monomers are also well-suited to obtain homogeneous copolymer materials; the copolymerization of hydrophobic and hydrophilic monomers leads to amphiphilic polymer particles. An overview of the many possibilities for radical polymerizations in miniemulsions are given in several reviews,<sup>[1–3]</sup> and some examples are shown in Figure 2a–c). The strength of the miniemulsion process is that it is not limited to radical polymerization; other types of polymerizations can also be carried out. Anionic polymerization can be used to obtain to

polyamide in non-aqueous miniemulsions,<sup>[4]</sup> and in the aqueous phase, owing to the reactivity of cyanoacrylates, poly(butyl cyanoacrylate)<sup>[5]</sup> nanoparticles (Figure 2d) can be synthesized by using different nucleophiles. Also the cationic polymerization of *p*-methoxystyrene<sup>[6,7]</sup> can be carried out in a miniemulsion. Catalytic polymerizations of monomer miniemulsions, in which polymerization occurs in the miniemulsion droplets to afford polymer nanoparticles, have been reported for the following reactions: the copolymerization of terminal olefins in a miniemulsion to form polyolefins,<sup>[8,9]</sup> the copolymerization of terminal olefin miniemulsions to polyketones,<sup>[10]</sup> the ring-opening metathesis polymerization of norbornene,<sup>[11,12]</sup> the homopolymerization of terminal olefins,<sup>[13]</sup> the polymerization of phenylacetylene,<sup>[14]</sup> and the step-growth acyclic diene metathesis (ADMET) polymerization of divinylbenzene in miniemulsions to give oligo(phenylene vinylene) particles.<sup>[15]</sup>

Polyaddition in miniemulsions lead to polyepoxide<sup>[16]</sup> and polyurethane<sup>[17]</sup> particles. In the case of the polyurethanes in an aqueous medium, the reaction with water has to be minimized, which can be achieved by the addition of a catalyst that allows create polyurethanes to be formed with high molecular weight.<sup>[18]</sup> Condensation and polycondensation processes in the presence of water appears to be contradictory terms, as in bulk processes it is known that high temperatures have to be applied and water has to be removed. However, in the heterophase, a locally high hydrophobicity in the droplets allows water to be expelled from the reaction locus. Saam et al. studied the polycondensation in suspension of hydrophobic diol and diacid compounds using different sulfonate surfactants;<sup>[19,20]</sup> however, stable latexes could not be obtained. In a miniemulsion, stable polyester<sup>[21]</sup> nanoparticles with a high yield in the polymerization reaction could be synthesized.

In a completely different process, Kobayashi et al. reported the synthesis of polyesters in the aqueous medium catalyzed with a lipase.<sup>[22–24]</sup> For example, the reaction of sebacic acid and 1,8-octanediol using *Pseudomonas cepacia* lipase in water yielded the corresponding polyester in 43 % yield with a molecular weight of 1600 g mol<sup>−1</sup>. Much higher molecular weight polyesters were obtained in miniemulsions with lactones catalyzed with the lipase *Pseudomonas sp.* (PS).<sup>[25]</sup> The polymerase chain reaction could also be successfully carried out in miniemulsions for DNA replication.<sup>[26]</sup> In this case, the parameters were chosen such that conditions for single-molecule chemistry were obtained, as the three-dimensional space is compartmentalized in small nanoreactors; in each compartment, the same reaction takes place in a highly parallel fashion on every DNA molecule.

The oxidative polymerization of aniline leads to polyaniline nanoparticles.<sup>[27,28]</sup> For catalytic polymerizations in the heterophase, the catalyst can be dispersed in small droplets in a miniemulsion. The monomer can then diffuse to the catalyst, where the reaction can take place to obtain polyethylene dispersions,<sup>[29–31]</sup> 1,2-polybutadiene,<sup>[32]</sup> or polyacetylene dispersions.<sup>[33]</sup>

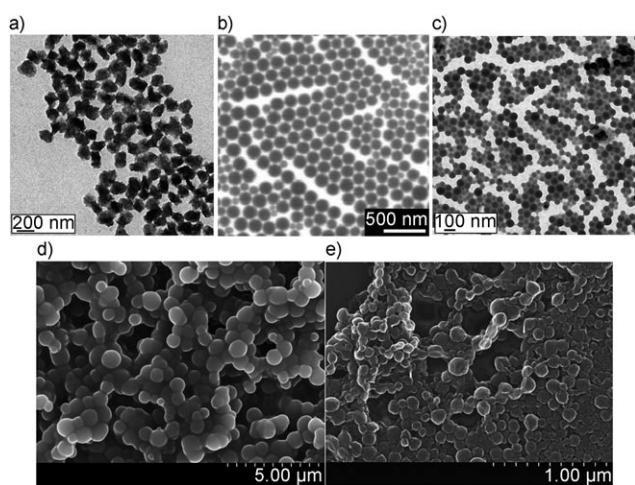


**Figure 2.** TEM (a–c) and SEM (d,e) images of a) polyacrylonitrile nanoparticles and b) polyisoprene nanoparticles as obtained by radical polymerization in direct miniemulsion; c) polyacrylamide nanoparticles as obtained by radical polymerization in inverse miniemulsion; d) poly-(butyl cyanoacrylate) nanoparticles as obtained by anionic polymerization; and e) PLLA particles as obtained by evaporation/miniemulsion techniques.



Katharina Landfester studied chemistry in Darmstadt and Strasbourg (Diplom, Prof. M. Lambla). She received her doctoral degree in 1995 from the University of Mainz under the supervision of Prof. H. W. Spiess (MPI for Polymer Research). After a post-doctoral stay at the Lehigh University (Bethlehem, USA, with Prof. M. El-Aasser), she joined the group of Prof. M. Antonietti at the MPI for Colloids and Interfaces (Golm), where she led the miniemulsions group. In 2002 she completed her habilitation in physical chemistry at the University of Potsdam. In 2003, she accepted a chair in macromolecular chemistry at the University of Ulm. She has been Director at the MPI for Polymer Research in Mainz since 2008.



## 2.2. Particle Formation with Preformed Polymers

Some polymers are more difficult to synthesize directly in the heterophase because, for example, special catalysts have to be used. Therefore, in some cases, a preformed polymer can be used for the preparation of polymeric nanoparticles. Such artificial latexes can be formed from the droplets consisting of a solution of the preformed polymer. After evaporation of the solvent, a polymer dispersion is obtained. This way, semi-conducting polymers, dissolved in organic solvents and miniemulsified in an aqueous phase using an adequate surfactant, were transferred to aqueous dispersions.<sup>[34]</sup> The combination of the emulsion/solvent evaporation method and the miniemulsion technique was also applied in the formulation of biodegradable nanoparticles using different biocompatible and biodegradable polymers, such as poly(L-lactide) (PLLA; see Figure 2e), poly(D,L-lactide-co-glycolide) (PLGA), and poly( $\epsilon$ -caprolactone) (PCL).<sup>[35]</sup> Differences in the results of various polymers are found in terms of the particle size and size distribution, and in the degradation time. It was also possible to create colloiddally stable lattices from low-molecular-weight ethylene-propylene-diene copolymers.<sup>[36]</sup>

## 3. Encapsulation of Soluble and Insoluble Materials

### 3.1. Soluble Materials

The miniemulsion polymerization technique also allows the preparation of highly uniform and practically monodisperse latex particles containing hydrophobic metal complexes, such as bis(acetylacetonato)platinum(II), tris(acetylacetonato)indium(III), bis(tetramethylheptadionato)zinc(II), bis(phthalocyanino)zinc(II), and tris(benzoylacetonato)chromium(III), each with different loading capacities.<sup>[37]</sup> The complexes are dissolved in the monomer prior to polymerization. In some cases, the homogeneity of the latexes was improved further by adapted emulsion techniques. With varying amounts of surfactant, the particle size can be tuned between 100 and 260 nm. Larger particles of up to 370 nm in size for a given metal complex were obtained by an additional feeding of monomer (Figure 3). The particles can further be used for nanolithography (see Section 10).

Whereas the above-mentioned transition-metal complexes are homogeneously distributed in the particles after polymerization, neutral, inert inner-shell lanthanoid complexes, such as  $[\text{Gd}^{\text{III}}(\text{tmhd})_3]$  (tmhd: 2,2,6,6-tetramethyl-3,5-heptanedionate),  $[\text{Eu}^{\text{III}}(\text{fod})_3]$  (fod: 1,1,1,2,2,3,3-heptafluoro-4,6-octandionate), or  $[\text{Ho}^{\text{III}}(\text{thmd})_3]$ , in combination with ester-containing monomers, such as butyl acrylate, leads after polymerization in miniemulsion droplets to the spontaneous formation of highly organized layered nanocomposite particles (Figure 4a).<sup>[38]</sup> The nanocomposite comprises a lanthanide complex phase and a polymer phase with a lamellar repeat period of about 3.5 nm, which is somewhat independent of the system composition. As the structure inside the particle can vary by changing the surfactant (Figure 4b), the

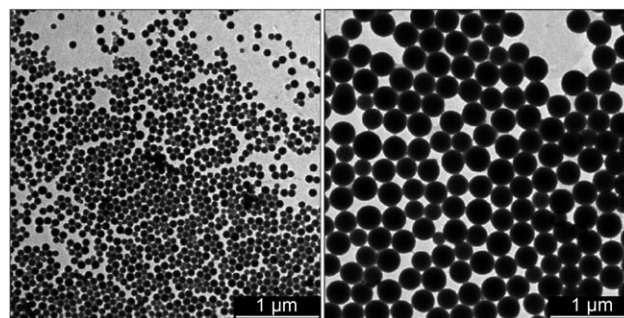


**Figure 3.** TEM images of platinum-complex-containing nanoparticles of different sizes (left: 105 nm; right: 370 nm).

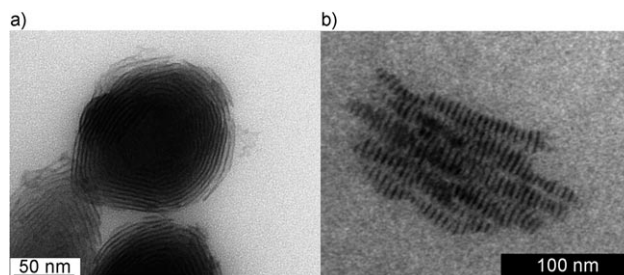


**Figure 4.** TEM images of polymer particles containing the hydrophobic gadolinium complex  $[\text{Gd}(\text{tmhd})_3]$  in combination with different surfactants: a) sodium dodecyl sulfate, b) sodium stearate.

interfacial substance also plays a role in the structure formation.

A hydrophobic fluorescent dye, for example as a marker for cell experiments, can be easily embedded in polymeric nanoparticles.<sup>[39]</sup> In this case, the dye molecules are molecularly dissolved in the monomer, and after polymerization homogeneously distributed in the polymer.

### 3.2. Insoluble Materials

The encapsulation of solids is more challenging. For the encapsulation of inorganic particles, such as colloidal silica,<sup>[40,41]</sup> titanium dioxide pigments,<sup>[42]</sup> and silver particles,<sup>[43]</sup> in a polymeric shell, the conventional emulsion polymerization can be used. Apart from the difficulty in controlling the dispersion stability of inorganic particles in the aqueous phase prior to polymerization, resulting in large aggregates, it is also difficult to exclusively polymerize the monomer on the surface of the nanoparticles; secondary nucleation often takes place and leads to insufficient encapsulation efficiencies. Differences in the diffusion behavior of relatively water-insoluble monomers from the monomer droplets to the growing polymerizing particles can cause variations in the copolymer composition. For the encapsulation of hydrophilic components, the surfaces have to be made hydrophobic by functionalization, which can be obtained with coupling agents, such as 3-(trimethoxysilyl)propyl methacrylate (MPS), through a surface chemical reaction.<sup>[41]</sup> MPS leads to an enhancement of the adsorption of nonpolar monomer and/

or polymer on the mineral surface, and provides a covalent attachment of polymer chains to the pigment surface with a polymerizable alkene group. Functionalization can also be performed through simple adsorption methods, for example by the adsorption of cationic initiators such as 2,2'-azobis(2-amidinopropane) dihydrochloride (AIBA·2HCl) onto negatively charged surfaces. The polymerization reaction of monomers can then be initiated by the attaching the AIBA initiator to titanium dioxide particles, for example.<sup>[42]</sup> Encapsulation can also be obtained using the dispersion polymerization technique. For example, MPS-coupled silica particles can be encapsulated with polystyrene in aqueous ethanol<sup>[44–46]</sup> and with poly (*tert*-butyl acrylate) in 2-propanol.<sup>[47]</sup>

Compared to emulsion and dispersion polymerization, miniemulsion polymerization offers several advantages. In a miniemulsion, the monomer droplets are small, so that the polymerization occurs by radical entry into the preexisting miniemulsion droplets without formation of new particles. As the generated homogeneous monomer droplets keep their particular identity during the polymerization without serious exchange kinetics being involved,<sup>[48]</sup> the polymer composition in the copolymerization for each particle reflects that of the corresponding monomers in the original droplets. The introduction of species such as pigments into the monomer prior to miniemulsification in the water phase, followed by polymerization, leads to high encapsulation efficiencies. Encapsulation of pigments or inorganic nanoparticles with polymers using the miniemulsion polymerization technique offers the ability to control the droplet size, having the pigment particles directly dispersed in the oil phase, and to nucleate all of the monomer droplets containing the pigment particles.

Using the miniemulsion approach, nanoparticles that are more hydrophobic than the monomer can be dispersed in the monomer phase without any former treatment, as recently described for the polystyrene encapsulation of organic phthalocyanine blue pigments<sup>[49]</sup> or carbon-black particles.<sup>[50]</sup> For the encapsulation of hydrophilic nanoparticles, such as calcium carbonate,<sup>[50]</sup> titanium dioxide,<sup>[51,52]</sup> magnetite,<sup>[53]</sup> fluorescent CdS/ZnS-coated CdSe<sup>[54]</sup> or CdS quantum dots,<sup>[55,56]</sup> montmorillonite,<sup>[57,58]</sup> silica,<sup>[59,60]</sup> silver,<sup>[61]</sup> or yttrium oxysulfide phosphorescent particles,<sup>[62]</sup> with hydrophobic polymers, hydrophobization of the inorganic nanoparticles is necessary prior to or during the introduction in the monomer phase. Calcium carbonate<sup>[50]</sup> and magnetite particles<sup>[53]</sup> can be successfully encapsulated into polystyrene particles using stearic acid and oleoyl sarcosine acid, respectively, as hydrophobizing agents. Erdem et al. used OLOA 370, a polybutene succinimide pentamine, for a successful dispersion of titanium dioxide nanoparticles into organic media.<sup>[51]</sup> The silver was made hydrophobic by carbon,<sup>[61]</sup> and the quantum dots could be functionalized with a trialkyl phosphine that was previously modified with an atom-transfer radical polymerization (ATRP) chlorine initiator.<sup>[55]</sup> Silica nanoparticles were made hydrophobic by cetyltrimethylammonium chloride (CTMACl) before dispersing them in hydrophobic monomers.<sup>[59]</sup> Hydrophobicity can also be obtained by alkoxyamine initiators based on *N-tert*-butyl-1-diethylphosphono-2,2-dimethylpropyl nitroxide that carry a terminal functional group, and which were synthesized in situ

and grafted to the silica surface. The resulting grafted alkoxyamines have been employed to initiate the growth of polystyrene chains from the inorganic surface.<sup>[63]</sup>

However, using the approach of dispersing the inorganic material directly into the monomer phase prior to miniemulsification, only a relatively low inorganic material content (<10%) can be obtained in the resulting nanocomposites, and its distribution is usually inhomogeneous, which is due to strong interactions and therefore clustering of the materials to be encapsulated.

Therefore, a new route for the production of polymer-encapsulated hydrophobic particles has been developed that is also based on miniemulsion processes. The co-sonication of two separately prepared dispersions, namely the nanoparticle dispersion and monomer miniemulsion, followed by a polymerization, leads to effective particle encapsulation (Figure 5). Using this method, hydrophobic carbon-black

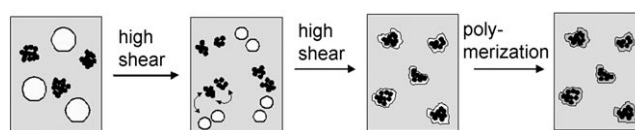


**Figure 5.** The co-sonication miniemulsion process for the encapsulation of hydrophobic or hydrophobized materials in polymeric nanoparticles. Monomer miniemulsion droplets and the hydrophobized material are dispersed separately. The application of high shear leads to the formation of droplets incorporating the hydrophobized material by fusion and fission processes. After subsequent polymerization, hybrid particles are obtained.

particles or other pigments can be encapsulated by polymers (e.g. polystyrene, polyacrylates, polyurethanes; Figure 6a) very efficiently, and the ratio of carbon black to polymer can

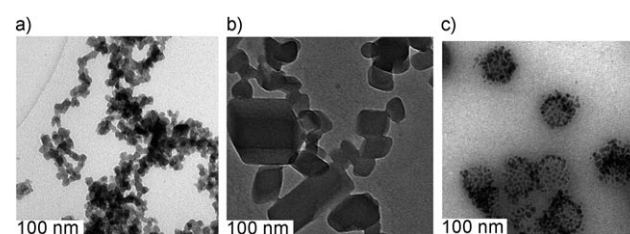


**Figure 6.** TEM images of the encapsulation of a) carbon black aggregates by polyurethane, b) azopigment colloids by polystyrene, and c) magnetite colloids by polystyrene.

vary over a wide range.<sup>[64]</sup> The polymerization can be described as polymerization in an adsorbed monomer layer created and stabilized as a miniemulsion (“ad-mini-emulsion polymerization”).

With the co-sonication method combining the corresponding pigment dispersion and a monomer miniemulsion, different organic pigment nanoparticles could be encapsulated efficiently with the polymer, resulting in hybrid structures with a pigment-to-polymer weight ratio of 80:20 (Figure 6b).<sup>[65]</sup> The successful encapsulation was shown by a

combination of analytic methods, including ultracentrifugation, electron microscopic methods, and streaming potential titrations at different pH values. Comparing the reaction kinetics of a typical styrene miniemulsion polymerization (in the absence of pigment) with corresponding ad-miniemulsion polymerizations proceeding on the surface of different pigment particles, a significant influence on the kind of pigment in terms of its molecular structure was detected. Considerably lower reaction rates could be attributed to the existence of the nitrobenzene fragment in pigment molecules retarding the reaction by acting as an effective scavenger. The remarkable inhibition period of the analogous reaction on other pigment surfaces was also attributed to its molecular structure. Pigment molecules with unsubstituted *trans*-quinacridones acted as strong inhibitors of polymerization reactions. Using the same encapsulation method, hydrophobized magnetite can be encapsulated by the same procedure, resulting in particles of high homogeneity with up to 40 wt% of magnetite (Figure 6c).<sup>[66]</sup>

### 3.3. Dual-Use Nanoparticles

Dual-use nanoparticles containing two reporters, namely a soluble fluorescent dye and insoluble magnetite nanoparticles, were synthesized in a three-step miniemulsion process.<sup>[67]</sup> The fluorescent dye is used for visualization by laser scanning microscopy *in vitro* (Figure 7a), and the magnetite (Figure 7b) for magnetic resonance tomography *in vivo*. The designing of the surface with defined amounts of carboxylic acid groups was achieved by copolymerization of the hydrophobic monomer styrene with acrylic acid. The magnetization measurements demonstrated that the paramagnetic behavior of the magnetic nanoparticles is maintained during polymerization, which means that the magnetite nanoparticles stay well-separated within the polymeric shell. It was shown that the uptake of these nanoparticles into different cells is dependent on the number of carboxylic groups on the surface. An increase of carboxylic surface groups leads also to a significant increase in the uptake behavior in endosomal compartments, as demonstrated by laser scanning microscopy and transmission electron microscopy. Further modification of the surface was achieved by physically adsorbing poly(L-lysine), or covalently coupling lysine to the surface. The positively charged transfection functionalities leads to a significantly increased uptake; the best uptake for the nanoparticles is obtained by the covalent lysine modification, for which high amounts of iron can be detected in the cells, thus making them suitable for a wide range of biomedical applications, such as use as a contrast agent for magnet resonance imaging, hyperthermia, and cell selection.

## 4. Encapsulation of Liquids

Nanocapsules can be formulated from a variety of synthetic or natural monomers or polymers by using different techniques to fulfill application requirements.

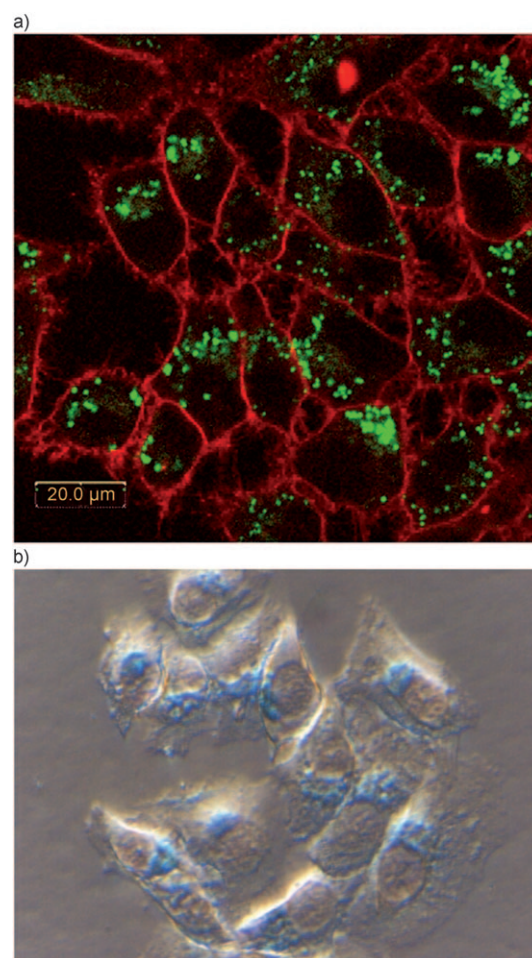


**Figure 7.** a) Laser scanning microscopy of HeLa cells. Cell membranes are stained with RH414 in red and the nanoparticles in green. b) Prussian-blue staining of nanoparticles in HeLa cells.

The encapsulation of peptides and proteins was achieved by the formulation of microcapsules using the double-emulsion technique,<sup>[68–70]</sup> emulsification/solvent evaporation, the diffusion method,<sup>[71–73]</sup> or the salting-out procedure.<sup>[74]</sup> A different approach is the layer-by-layer technique, which was used to form nanocapsules by using a template as core onto which alternately positively and negatively charged polyelectrolyte layers can be added.<sup>[75]</sup> For example, melamine formaldehyde as the sacrificial core and poly(allylamine hydrochloride) and poly(acrylic acid) sodium salt as electrolytes were used.<sup>[76]</sup> Poly(ethyleneimine) microcapsules can also be prepared by the glutaraldehyde-mediated covalent layer-by-layer assembly method, which cross-links the adsorbed poly(ethyleneimine) layer and introduces free aldehyde groups on the surface for the next PEI adsorption on  $\text{MnCO}_3$  microparticles, followed by core removal.<sup>[77]</sup> Covalently stabilized hollow capsules from biodegradable materials can also be obtained using a combination of click chemistry and layer-by-layer assembly.<sup>[78]</sup>

Various miniemulsion-based methods for the encapsulation of liquids are summarized in Figure 8 and will be discussed in Sections 4.1 and 4.2.



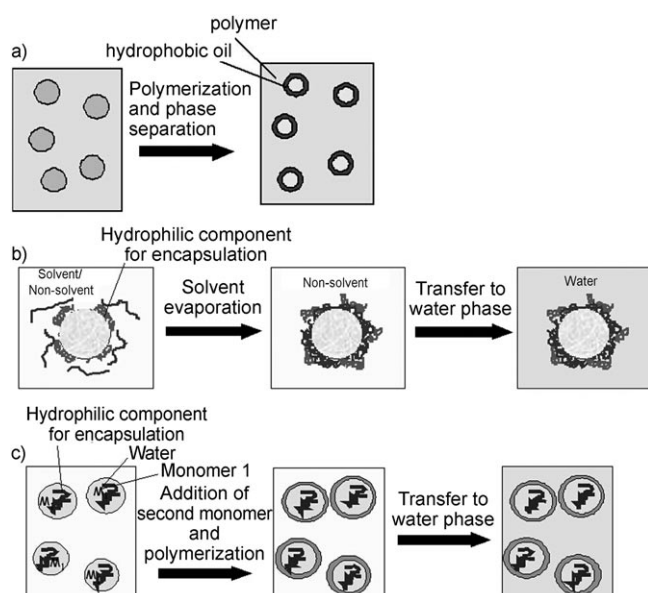


**Figure 8.** Formation of nanocapsules. a) Phase separation during polymerization: before polymerization, the monomer and the hydrophobic oil form a homogeneous droplet phase, and polymerization phase separation occurs, leading to the formation of nanocapsules. b) Nano-precipitation: an inverse miniemulsion is formed with the hydrophilic component for encapsulation inside the aqueous droplets; the continuous phase consists of a solvent/non-solvent mixture for the polymer. During evaporation of the solvent, the polymer precipitates onto the nanodroplets, thus forming the nanocapsules, which can subsequently be transferred to the water phase. c) Interfacial polymer reaction on miniemulsion droplets: droplets in an inverse miniemulsion contain the hydrophilic component for encapsulation and monomer 1; addition of the second monomer via the continuous phase leads to a polymerization at the interface, thus forming the nanocapsules, which can be transferred to the water phase.

#### 4.1. Hydrophobic Liquids

Throughout the polymerization process, phase separation can be used for the synthesis of hollow polymer nanocapsules as a convenient one-step miniemulsion process. The nanocapsules are formed by a variety of monomers in the presence of larger amounts of a hydrophobic oil. The monomer and hydrophobic oil first form a common miniemulsion before polymerization, by which the polymer is immiscible with the hydrophobic oil and phase-separates throughout polymerization to form particles with a morphology consisting of a hollow polymer structure surrounding the hydrophobic oil.

The effect of different monomers and monomer mixtures, of the type and amount of surfactant, and of the hydrophobic oil hexadecane on the morphological characteristics of the polymer/oil composite particle has been studied.<sup>[79]</sup> The differences in the hydrophilicity of the oil and the polymer turned out to be the driving force for the formation of nanocapsules. In the case of poly(methyl methacrylate) (PMMA) and hexadecane, the pronounced differences in hydrophilicity are suitable for direct nanocapsule formation. For styrene as monomer, the hydrophilicity of the polymer phase has to be adjusted by surfactants or the addition of co-

monomers to favor nanocapsule structure formation (Figure 9a).

An encapsulation by phase separation was effective in the case of polymerizing a monomer in the presence of a solid photoinitiator (Figure 9b).<sup>[80]</sup> A solution of the photoinitiator in monomer was miniemulsified in water, followed by a polymerization process in which phase separation of the photoinitiator and the formed polymer led to amorphously solidified photoinitiator nanoparticles encapsulated by polymer.

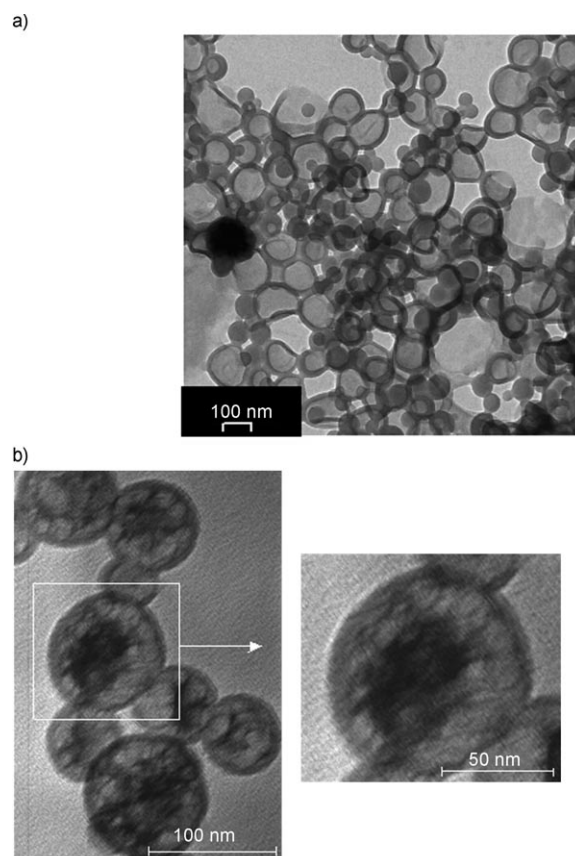


**Figure 9.** TEM images of a) nanocapsules consisting of styrene, the co-monomer acrylic acid, and hexadecane as hydrophobic oil after the phase separation process, and b) encapsulation of a photoinitiator by a PMMA shell.

The fragrance 1,2-dimethyl-1-phenyl-butylamide was embedded in different polymer nanoparticles, also using the miniemulsion technique.<sup>[81]</sup> The combination of transmission electron microscopy and calorimetric experiments suggest that the particles consist of a matrix composed of the fragrance in the polymer up to about 25 % of the fragrance; only at larger quantities of the fragrance, small microdomains are probably formed, which are homogeneously located in the particle.

Amphiphilic oligomers of styrene and maleic acid were used for a nanoencapsulation by interfacially confined controlled/living radical miniemulsion polymerization. The oligomers can adsorb at the water/droplet interface, allowing

a radical addition–fragmentation chain transfer (RAFT) living polymerization at the interface.<sup>[82]</sup>

## 4.2. Hydrophilic Liquids

### 4.2.1. Interfacial Polymerization

Interfacial reactions are one of the most well-established methods in the preparation of nanocapsules. Nanometer-sized hollow polymer particles were synthesized by employing such interfacial cross-linking reactions as polyaddition and polycondensation (Figure 8b),<sup>[83–86]</sup> radical,<sup>[87,88]</sup> or anionic polymerization.<sup>[89,90]</sup> It is also possible to prepare nanocapsules by miniemulsifying the disperse phase, namely a solution of nylon 6 in formic acid, in cyclohexane. Methanol is then added to the miniemulsion, which immediately reacts with the formic acid. The product of the reaction, methyl formate, is evaporated, and water replaces the formic acid in the droplets, thus allowing the precipitation of nylon 6 at the interface of the droplets, resulting in the formation of nanocapsules.<sup>[91]</sup>

**Polyaddition:** Functional hollow nanoreactors with a hydrophilic liquid core can be obtained by interfacial polycondensation or cross-linking reactions in an inverse miniemulsion. By varying the monomers, polyurea, polythiourea, and polyurethane nanocapsules can be formed.<sup>[83]</sup> As nanocapsules composed of biocompatible and biodegradable materials are of growing interest for the use as markers and drug-delivery systems in the human body, nanocapsules consisting of cross-linked potato starch with encapsulated DNA molecules have recently been prepared. Solutions of amines or alcohols in a polar solvent were miniemulsified in a non-polar continuous phase. The addition of suitable hydrophobic diisocyanate or diisothiocyanate monomers to the continuous phase allows the polyaddition or the cross-linking reactions to take place at the interface of the droplets. The resulting polymer nanocapsules could be subsequently dispersed in water.

The polyaddition of the chitosan stabilizer with two biocompatible costabilizers, Jeffamine D2000 and Gluadin, and a linking diepoxide in presence of an inert oil results in thin but rather stable nanocapsules via an interface reaction on miniemulsion droplets.<sup>[92]</sup> As both water- and oil-soluble aminic costabilizers can be used, these experiments lead the way to a great variety of capsules with different chemical structures. These capsules are expected to be biocompatible and biodegradable, and they may find applications in drug delivery (Figure 10a).

Different components can be encapsulated in the nanocapsules that act as independent nanoreactor; for example, silver nitrate was encapsulated and subsequently reduced to give silver nanoparticles inside the nanocapsules (Figure 10b).<sup>[83]</sup> The capsules can also contain a gadolinium complex (Magnevist, GdDTPA (DTPA = diethylenetriaminepentaacetate); Gadovist) as contrast agent surrounded by a shell, which is highly permeable to water, allowing almost free exchange with the bulk water (Figure 10c).<sup>[93]</sup> In comparison with the non-encapsulated contrast agent,  $T_1$  relaxivity measurements using NMR spectroscopy revealed a slight decrease of relaxivity in water and in human blood after

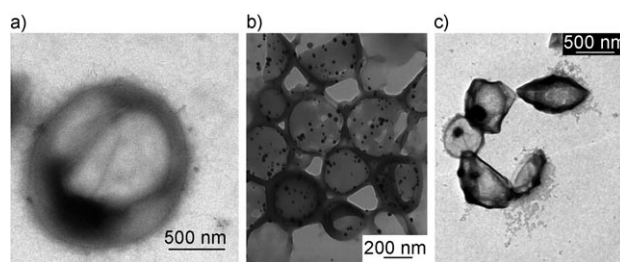


**Figure 10.** TEM images of nanocapsules as obtained by an interfacial polyaddition reaction. a) Chitosan nanocapsules; b) polyurethane nanocapsules with encapsulated silver salt that was subsequently reduced after capsule formation; c) polyurethane capsules loaded with a contrast agent, the gadolinium complex GdDTPA.

encapsulation of Magnevist. As the limiting factor for targeted contrast agents is the number of local receptor sites, the local relaxivity is governed by the number of bound capsules. Considering the high possible gadolinium load of a single capsule of between roughly  $10^{-17}$  mmol (50 nm) and  $10^{-14}$  mmol (300 nm) while at least maintaining the relaxivity of the embedded agent, the possible enhancement per binding site is significantly boosted compared to conventional paramagnetic extracellular contrast agents. The suggested approach appears not to be limited to the encapsulation of Magnevist, as shown by the Gadovist example, and can most likely act as a new basis for versatile contrast agents in MRI.

**Radical Polymerization:** Aqueous-core capsules with uniform polymeric shells could also be prepared by using the free-radical polymerization process. The reaction was constrained to the interface of water-in-oil spheres by the alternating copolymerization of hydrophobic maleate esters and hydrophilic poly(hydroxy vinyl ether)s. In these polymerizations, the kinetics, shell thickness, and release characteristics of the resulting aqueous-core capsules are set by the diffusion-limited alternating reaction of the oil-soluble maleate esters and water-soluble vinyl ethers.<sup>[94]</sup>

**Anionic polymerization:** Apart from a polyaddition reaction at the interface, anionic polymerization can also be carried out. Monodisperse biodegradable poly(*n*-butyl cyanoacrylate) nanocapsules containing DNA molecules with 790 base pairs in an aqueous core could be prepared by anionically polymerizing *n*-butyl cyanoacrylate at the droplet interface in an inverse miniemulsion.<sup>[95]</sup> The aqueous droplets in the size range of 300–700 nm dispersed in the hydrophobic continuous phase were formulated using the miniemulsion technique, which allows an easy control of the droplet size and size distribution. The thickness of the capsules can be tuned by the amount of butyl cyanoacrylate used for the synthesis (Figure 11). After polymerization, the capsules were transferred to an aqueous phase. Independent of the surfactant type, the encapsulation efficiency of DNA was about 100%. At least 15 % of the total DNA was found to be in the form of free undisturbed double helix chains, as determined by resolved agarose gel electrophoresis.



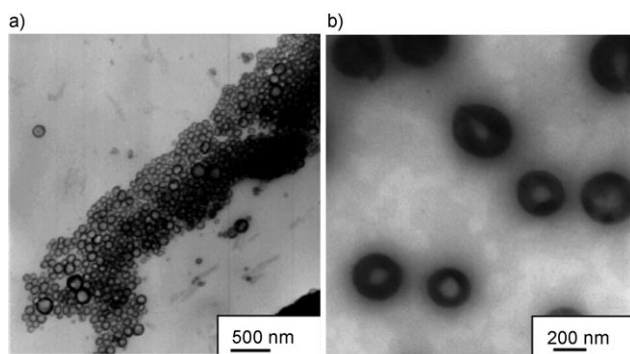


**Figure 11.** TEM images of poly(*n*-butylcyanoacrylate) (PBCA) capsules obtained in the presence of 5 wt % polysorbate 80 (Span80) and a) small and b) large amounts of the monomer butyl cyanoacrylate.

#### 4.2.2. Nanoprecipitation

As another possibility for the formation of nanocapsules is a nanoprecipitation of preformed polymers onto miniemulsion droplets. For example, by interfacial deposition of the preformed polymer, poly(D,L-lactide)-based nanocapsules containing an antitumoral agent<sup>[96]</sup> or poly(methyl methacrylate) capsules with an entrapped antiseptic agent<sup>[97]</sup> were successfully prepared. The modified nanoprecipitation of polymers onto stable nanodroplets with an antiseptic agent has been successfully applied for the preparation of well-defined nanocapsules.<sup>[97]</sup> Stable nanodroplets of a chlorhexidine digluconate aqueous solution were obtained by inverse miniemulsions in a mixed solvent/nonsolvent organic medium containing an oil-soluble surfactant and the polymer for the shell formation. A change of gradient of the dichloromethane/cyclohexane solvent/nonsolvent mixture led to the precipitation of the polymer in the organic continuous phase and deposition onto the large interface of the miniemulsion aqueous droplets. The size of the polymer nanocapsules could be adjusted by varying the amount of the surfactant within a size range of 80–240 nm. The nanocapsules could be easily transferred into water as a continuous phase, resulting in aqueous dispersions with nanocapsules containing an aqueous core with the antiseptic agent. The quantity of encapsulated antiseptic agent was evaluated to indicate the durability of the nanocapsule wall. Furthermore, the use of different polymer types in this process (e.g. poly( $\epsilon$ -caprolactone)); Figure 12) with glass transition temperatures ( $T_g$ ) ranging from 10 to 100 °C has been also successful.

#### 4.2.3. Inorganic Layers

Nanocapsules with a low permeability were obtained by thin layers of a crystalline material, which can be surface-bound to cationically charged miniemulsion droplets that serve as templates.<sup>[98]</sup> The single-crystalline building blocks forming the capsule then were glued and sealed by a subsequent chemical reaction. As a model system, a fully crystalline synthetic magnesium silicate with high structural uniformity and homogeneity was chosen with a thickness of 1.25 nm and a diameter of 28 nm. If a monomer is used for the

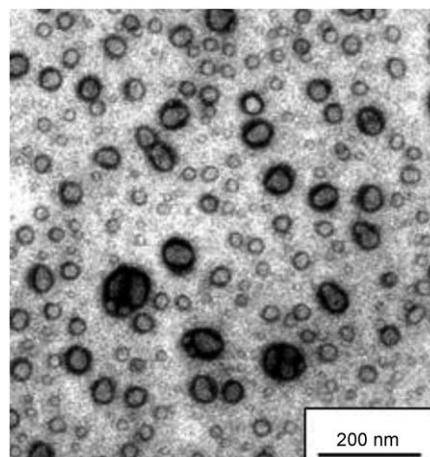


**Figure 12.** TEM image of the encapsulation of a hydrophilic antiseptic agent by nanoprecipitation in an inverse miniemulsion.

droplet formation, the sequential polymerization and encapsulation leads to “armored” latexes in which a polymer nanoparticle is completely covered with clay plates or scales, and film formation or coalescence is thus prevented (Figure 13). Such “armored latexes” are expected to be of interest as pressure-sensitive adhesives or as a new type of filler with unconventional chemical and mechanical performance.

### 5. Phase Separation of Polymers inside Particles

Most polymers do not mix, and therefore phase separation takes place. In the case of nanoparticles, phase separation is limited to the volume of the nanoparticle itself. Phase separation has already been discussed in Section 4.1 for the formation of nanocapsules. In that case, one component was a low-molecular-weight component and one a polymer. Phase separation of polymers within a polymer particle can lead to different morphologies. For the preparation of the nanoparticles in miniemulsion, either preformed polymers are

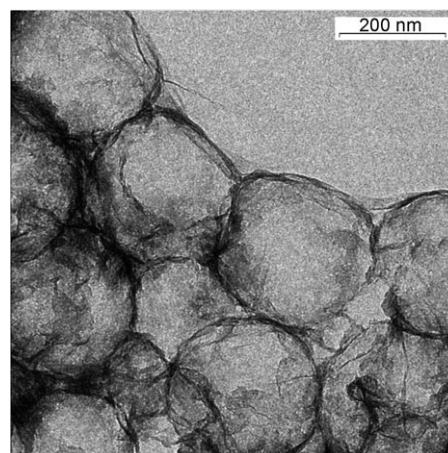


**Figure 13.** TEM image of hollow silica nanocapsules with a poly(methyl methacrylate) (PMMA) template.

used, a polymerization of different monomers takes place, or a polymer is dissolved in a monomer.

### 5.1. Particles from Droplets with a Solution of Preformed Polymers

For the preparation of nanoparticles with preformed polymers, the polymers are dissolved in a common solvent, and the homogeneous polymer solution is subsequently miniemulsified with an adequate surfactant in a continuous phase that is immiscible with the solvent. The solvent is then evaporated, resulting in polymer particles. If the two polymers are immiscible in each other (which is for most polymer combinations the case), phase separation takes place throughout the evaporation process. The morphology is driven by the type of the polymers, but also by the interfacial tensions between the phases, which can easily be varied, for example by the addition of surfactant, copolymers, and so on. The phase separation can be effectively visualized by using transmission electron microscopy (TEM; Figure 14). Blend particles consisting of polystyrene and poly(propylene carbonate) that formed from the two immiscible polymers by the

miniemulsion process exhibits biphasic morphologies.<sup>[99]</sup> The fact that no core-shell-type, but rather Janus-like structures were found indicates that the interaction between the solution–water interface (including the surfactant molecules) and each of the polymer phases is similar, and that there is no preference of only one polymer to the water phase. In addition to the TEM experiments, photoluminescence (PL) measurements were also performed. Both the TEM studies and the PL experiments provide strong evidence that phase separation and composition of the phases in these particles strictly follows the Flory–Huggins theory. This result highlights the applicability of the nanoparticle approach to either fabricate blend systems with well-controllable properties or to study structure–property relationships under well-defined conditions. For the PFB–F8BT blend (PFB = poly(9,9'-dioctylfluorene-*co*-bis-*N,N'*-(4-butylphenyl)bis-*N,N'*-phenyl-1,4-phenylenediamine), F8BT = poly(9,9'-dioctylfluorene-*co*-benzothiadiazole)), it could be shown that the PFB-rich phase contains F8BT at a concentration of only about 15 %, whereas the concentration of PFB in the F8BT-rich phase is even smaller, being between 5 and 10 %.

It is known that polymer layers can exhibit significantly improved performances if they possess a multicomponent phase-separated morphology. Two miniemulsion-based approaches were therefore compared for the formation of films by nanoparticles.<sup>[100,101]</sup> In the first approach, heterophase solid layers were prepared from an aqueous dispersion containing nanoparticles of two polymers, whereas in the second approach, both polymers are already contained in each individual nanoparticle. In both cases, the upper limit for the dimension of phase separation is determined by the size of the individual nanoparticles, which can be adjusted down to a few tens of nanometers. It was shown that the efficiencies of solar cells using two component particles are comparable to those of devices prepared from solution at comparable illumination conditions, and that they independent of the solvent used in the miniemulsion process.

### 5.2. Particles from Droplets with Monomers and Polymers

Instead of using a solvent for dissolving the polymers, a monomer can also be used in combination with a preformed polymer. The polymer–monomer solution can then be miniemulsified in water, and the monomer can subsequently be polymerized, resulting in phase-separating hybrid particles. For such a system, polycondensates, such as polyester, polyurethane, alkyd resin or epoxy resin, are usually dissolved in radically polymerizable monomer(s) before miniemulsification; a review is given by Guyot et al.<sup>[102]</sup> In the miniemulsion polymerization carried out with acrylic monomers in the presence of alkyd resins,<sup>[103,104]</sup> a retardation by the alkyd was reported; the limited monomer conversion could be improved by high polymerization temperatures and mixed (oil and water-soluble) initiators. The presence of two glass transition temperatures indicates that at least two phases, namely the poly(acrylate-*graft*-alkyd) and polyacrylate phase.

Tsavalas proposed a physical mechanism in which the more hydrophobic alkyd phase-separates into the core upon

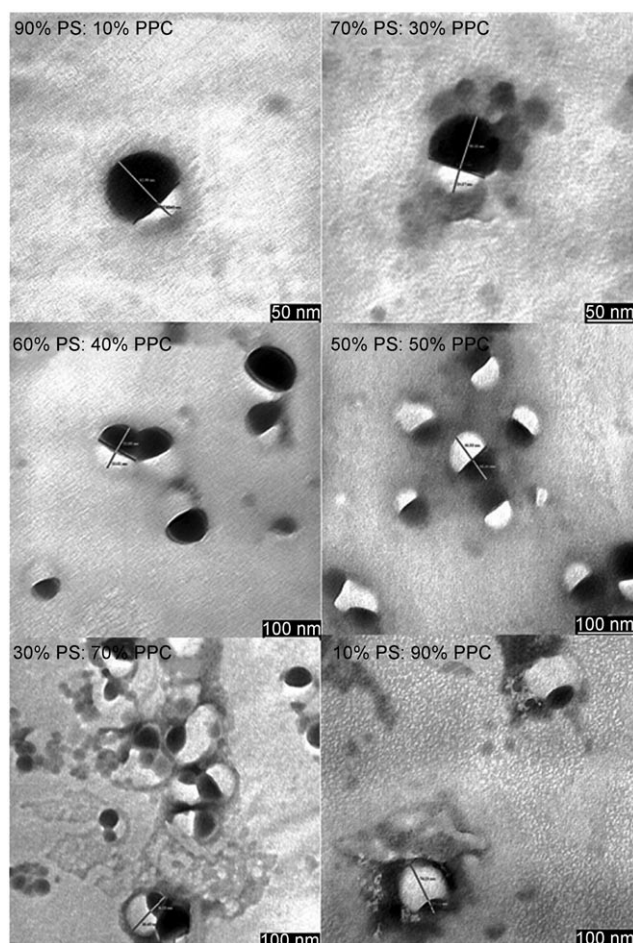


**Figure 14.** TEM images of phase separation inside nanoparticles at different ratios of polystyrene (PS; dark) to poly(propylene carbonate) (PPC; light).

polymerization, whereas the less hydrophobic polyacrylate forms a shell.<sup>[105]</sup> In the case of polymerizing butyl acrylate (BA) in the presence of alkyd, at the beginning of the reaction, BA monomer is thought to be dissolved in small alkyd domains distributed throughout a continuous BA particle phase. These islands eventually act as reservoirs, diffusing monomer to the polymerization of BA in the continuous particle phase.

Tsavalas also showed that the choice of monomer(s) is the most important variable in determining the level of grafting, which directly influences the phase separation. Therefore, differences in particle morphologies between acrylates and methacrylates could be shown that were attributed to different grafting possibilities.<sup>[106]</sup> The grafting is lower in the case of using methacrylates, as chain transfer dominates the interaction of methacrylate with resin. Conversely, the interaction of acrylate with resin is dominated by direct addition to a resin double bond, which is a highly efficient mode of grafting.

Miniemulsion polymerization with a three-component acrylic system consisting of methyl methacrylate, butyl acrylate, and acrylic acid (AA)<sup>[107]</sup> was carried out in the presence of an unsaturated polyester resin. A high level of cross-linking (over 70 %) was observed during polymerization in this particular hybrid system, in contrast to those involving alkyd as reported above. Electron microscopy showed the hybrid particle morphology to have internal domains of polyester resin in an acrylic matrix.

Gooch et al.<sup>[108]</sup> carried out hybrid miniemulsion polymerization with acrylic monomers (MMA, BA, and AA) in the presence of oil-modified polyurethanes (OMPU). Li et al.<sup>[109]</sup> used hybrid miniemulsion polymerization to prepare urethane/BMA latexes (BMA = butyl methacrylate) with particle sizes of about 50 nm. Blends prepared from these particles show evidence of phase separation.<sup>[110]</sup> Better homogeneity of the hybrids leads to improved elastomeric mechanical properties, which can be obtained by the hybrid miniemulsion polymerization of acrylate in the presence of linoleic acid and sunflower seed oil.<sup>[111]</sup>

### 5.3. Particles from Monomer Droplets

As a further possibility, two or more monomers can be used for the formation of droplets, which can then be polymerized. Miniemulsification of the mixed monomer species allowed efficient copolymerization reactions of fluorinated monomers with standard hydrophobic and hydrophilic monomers in a joint heterophase situation, resulting either in phase-separating block copolymers to form core-shell latexes, or statistical copolymers with more homogeneous particles. Contrary to the purely fluorinated polymers, those copolymers dissolve in organic solvents but still show the advantageous interface properties of the fluorinated species.<sup>[112]</sup>

Using monomers for a polyaddition and monomers for radical polymerization in one droplet allowed the combined synthesis of polyaddition and free radical polymerization in the same particle.<sup>[113]</sup> Hybrid particles were prepared by polymerizing isophorone diisocyanate with dodecanediol to

form polyurethane at the same time that the polystyrene or poly(butyl acrylate) was free radically polymerized. Neither intra- nor interparticle phase separation could be detected by TEM; the particles appeared to be homogenous.

Poly(siloxane acrylate) and poly(siloxane urethane) latexes with small and narrowly distributed particle sizes were synthesized by combining different polymerizations within the nanoparticles.<sup>[114]</sup> Poly(siloxane acrylate) latexes were obtained in a radical polymerization process. In this case, a copolymerization with other vinylic monomers is easily possible, leading to highly cross-linked copolymer particles. Owing to the confinement of the reaction within the minidroplets, the monomers are forced to copolymerize on the length scale of the droplets, and the phase separation is limited to the size of the particles.

Poly(siloxane urethane) nanoparticles could be obtained in a polyaddition process using a diisocyanate and silanediols. Replacing parts of the siloxanediol segments with a low glass transition temperature by alkyldiols allowed the introduction of crystalline parts in the material with higher melting points. However, these alkyldiols have to be sufficiently hydrophobic so that they do not interfere with the miniemulsion process. Hybrid particles can also be obtained on the base of those systems by additionally using styrene or an acrylate in the miniemulsification process. Although performed in a one-pot reaction after the miniemulsification step, the two polymer reactions take place consecutively. In the first reaction step, the poly(siloxane urethane) forms; the radical polymerization of the vinyl monomer takes place afterwards. By using hydroxymethyl methacrylate as a coupler, the two different polymers can be efficiently linked, and hybrid graft copolymers are formed.

A suppression of the phase separation within polyurethane-polystyrene nanoparticles could be obtained by synthesizing waterborne poly(urethane-*block*-styrene) latexes in an miniemulsion polymerization in only one batch.<sup>[115]</sup> A direct miniemulsion of the monomer mixture containing styrene, isophorone diisocyanate, 2,4-diethyl-1,5-pentanediol, and a diol-functionalized azoinitiator was prepared in water. In the first step, the polyaddition reaction of the polyurethane was then performed at room temperature, yielding a polyurethane macroazoinitiator. In a second step,

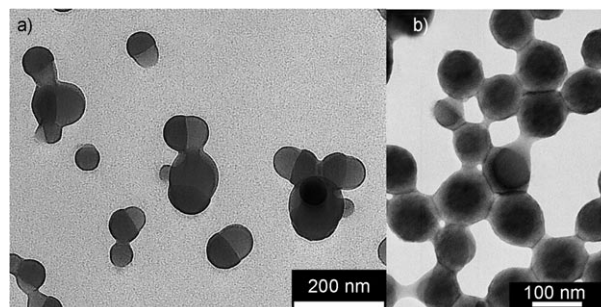


**Figure 15.** TEM images of the particles in miniemulsions after staining with  $\text{RuO}_4$ . The dark domains represent polystyrene, whereas the lighter domains are attributed to polyurethane (PU). a) Hybrid PS-PU homopolymer miniemulsion; b) hybrid PS-PU copolymer miniemulsion.



the radical polymerization of styrene was started from the macroazoinitiator chains by increasing the temperature. It was shown that 45 % of a (linear) copolymer consisting of a polyurethane and polystyrene was obtained, which turned out to be a good compatibilizer for polyurethane/polystyrene polymer blends to suppress the phase separation within the nanoparticles. TEM from the polymer particles in a miniemulsion revealed a homogeneous structure inside the particles (Figure 15).

## 6. Functionalization of Nanoparticles and Nanocapsules

### 6.1. Copolymerization

Carboxyl- and amino-functionalized polystyrene particles with defined amounts of the functional groups on the surface were synthesized by miniemulsion copolymerization.<sup>[39]</sup> The number of functional groups on the surface and the particle size can be controlled by the fraction of the functional monomer in the reaction mixture. Significant differences were observed between poly(St-co-AA) and poly(St-co-AEMH) particles (St = styrene, AEMH = aminoethylmethacrylate hydrochloride). An increase of the acrylic acid fraction leads to larger particles, whereas with increasing AEMH, smaller particles were obtained. Composite particles in the size range 100–150 nm for AA as a co-monomer and from 120 to 175 nm for AEMH were synthesized. Owing to the “hairy” layer formation, the amount of surface carboxyl groups on poly(St-co-AA) latex particles is three-and-a-half times higher than the amino groups on the surface of poly(St-co-AEMH) particles. To use the nanoparticles as markers for cells, a defined quantity of a fluorescent dye was also embedded in the nanoparticles. The particles could be used for the uptake experiments into cells. It is shown that the uptake increases with increasing surface charges, especially in the case of amino functionalization.

In the case of anionic polymerization of butylcyanoacrylate in a miniemulsion, a functionalization can be obtained by using functionalized nucleophiles to start the polymerization.<sup>[5]</sup> The nanoparticles were then used for cell uptake experiments. The molar mass of the polymer determines the onset of apoptosis, and total uptake is determined by the functionalization of the particles.<sup>[116]</sup> Different uptake kinetics were obtained with HeLa and Jurkat cells after incubation with the same particle batch. Interestingly, the intracellular particle distribution, visualized by confocal laser scanning microscopy, does not show significant differences for either of the cell lines or particle batches.

It is of particular interest that polysorbate-80-functionalized poly(*n*-butyl cyanoacrylate) (PBCA) nanoparticles provide direct evidence from *in vivo* experiments for the presence of nanoparticles entering the brain and the retina of rats, suggesting a passage through the blood–brain and blood–retina barriers.<sup>[117]</sup> This result makes such nanoparticles potential candidates for drug targeting systems in the brain.

### 6.2. Functionalization of Nanocapsules

The functionalization of well-defined polyurethane nanocapsules with an aqueous core, which were prepared by performing a polyaddition at the interface of inverse water-in-oil miniemulsion droplets, could be obtained by two methods: The carboxy- and amino-functionalized surface of the nanocapsules can be tailored by an *in-situ* carboxymethylation reaction (Figure 16a) or by physical adsorption of a cationic

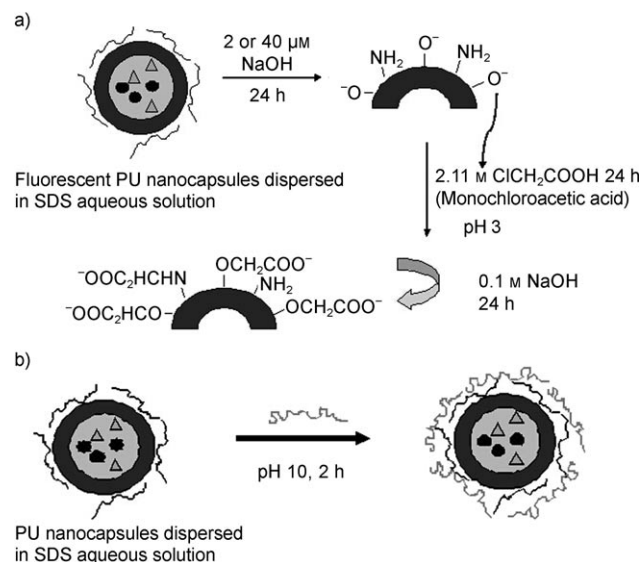


**Figure 16.** a) Carboxymethylation reaction for the functionalization of PU nanocapsules; b) Adsorption of poly(aminoethyl methacrylate) (PAEMA) or poly(ethyleneimine) (PEI) onto PU nanocapsules. SDS = sodium dodecylsulfate.

polyelectrolyte; that is, poly(aminoethyl methacrylate hydrochloride) or poly(ethyleneimine) (Figure 16b).<sup>[118]</sup> The increased uptake of amino-functionalized fluorescent nanocapsules by HeLa cells clearly demonstrates the potential of the functionalized nanocapsules to be successfully exploited as biocarriers.

## 7. Release from Nanocapsules

In some types of nanocapsules, it might be desirable to encapsulate the materials permanently, as for example in pigments for coatings. However, in many cases, a release of the encapsulated material is of interest, either over a long period of time or in an instant. Different approaches have to be chosen to fulfill the requirements of release kinetics.

### 7.1. Diffusion

Release of an encapsulated species can be obtained simply by a diffusion process from nanocapsules. It was shown that the release behavior of a copolymeric acrylic matrix with different amounts of encapsulated volatile fragrance is

significantly decelerated compared to the pure fragrance miniemulsion. For temperatures significantly lower than the glass transition temperature of the polymer ( $T < T_g$ ),<sup>[81]</sup> almost no release can be observed. An increase in the temperature to around and well above the transition temperature ( $T > T_g$ ) results in an slightly or significantly accelerated release of the fragrance out of the nanoparticles, respectively (Figure 17). Thereby, the release behavior of the volatile compound can be easily tuned by adjusting the release temperature in comparison to the glass transition temperature of the polymer shell.

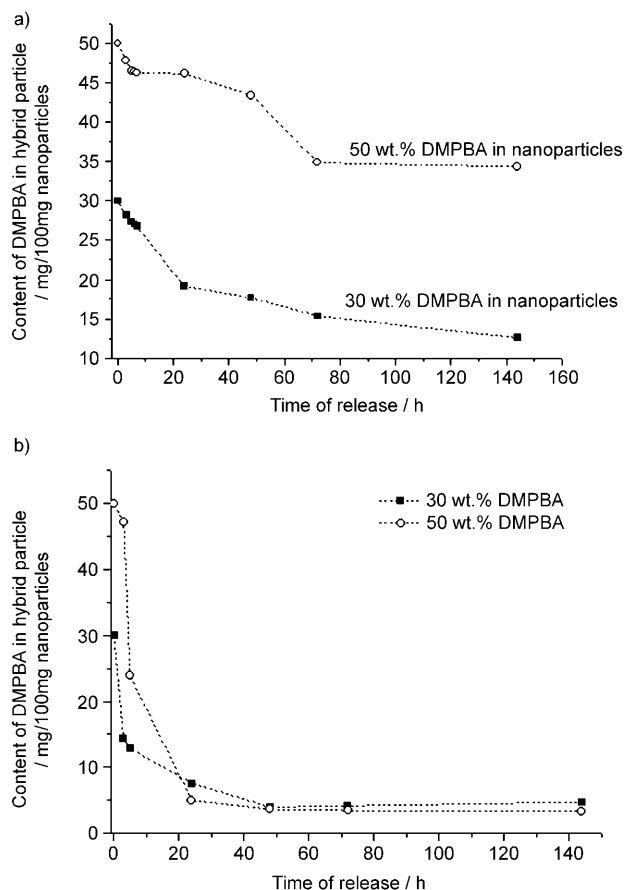


**Figure 17.** Release of the fragrance 1,2-dimethyl-1-phenyl-butylamide (DMPBA) at a) 55°C and b) at 90°C. No release is detected at room temperature.

For photoinitiator nanocapsules encapsulated in different polymeric shells, it was shown that the capsules are permeable and thus release the initiator in a sufficiently high concentration into the surrounding (monomer) phase to start the polymerization, even after a longer period of time.<sup>[80]</sup> The release rates clearly vary with the kind of the polymer shell and the employed redispersing agent. Studies of the kinetics show the great potential of these capsules for applications in polymeric dental filling materials as initiator depots to guarantee the required storage time.

## 7.2. Nanoexplosions

Another possibility of release is a sudden but controlled release of the encapsulated material by using switches in the shell materials that are sensitive to factors such as light or temperature. One possibility is to embed intact azoinitiators by radical polymerization in miniemulsion droplets at low reaction temperatures.<sup>[119]</sup> In spite of the thermal initiation of the polymerization process with a first azoinitiator decomposing at low temperatures, the embedded second azoinitiators maintain their character so that they can be detonated at a later time at higher temperatures. The nanoexplosion temperature has to be chosen below the glass transition temperature of the polymer so that the nitrogen gas which develops during the thermal treatment of the particles (caused by the decomposition of the encapsulated azoinitiator) builds up an overpressure on the inside of the particles and affects a blow-out by which the polymer surface is damaged (Figure 18). This concept allows a sudden release of

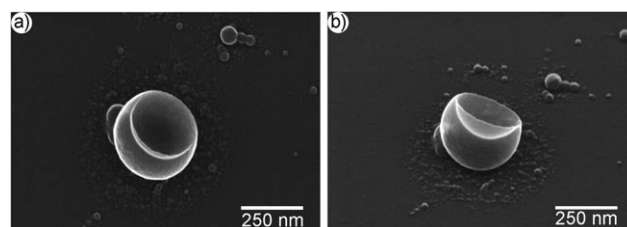


**Figure 18.** SEM image of nanocapsules with encapsulated azoinitiator after nanoexplosion at elevated temperatures: a) top view; b) viewing plane tilted by 45°.

materials that are also encapsulated in the particles. The concept can easily be transferred to other “explosives”, for example, redox initiators that function at lower temperatures, which liberate a gas inside polymeric particles during decomposition.

## 8. Structure Formation of Inorganic Nanoparticles

For the generation of colloid anatase nanoparticles, the sol–gel approach is of particular interest, which includes the controlled hydrolysis and condensation of appropriate precursors, which are usually titanium alkoxides. As the photocatalytic activity of anatase increases with smaller particle size, high porosity, high specific surface area, and a high degree of crystallinity, obtaining pure anatase at low processing temperatures with both a small grain size and a high degree of crystallinity is desired. However, the precipitates obtained by sol–gel processing are usually porous and amorphous. To induce a transition from the amorphous to the anatase phase, an annealing temperature higher than 300°C is generally required, leading to a collapse of the pore system and an increase of the particle size. A synthesis of crystalline titania at temperatures below 100°C<sup>[120]</sup> led in most cases to materials which have no porosity or high specific surface areas. Combining the sol–gel process with the

principles of liquid crystal templating, mesoporous materials can be synthesized. Using alkyl phosphate surfactants or dodecylamine as templates allowed the synthesis of mesoporous titania<sup>[121,122]</sup> with high specific surface areas of up to  $700 \text{ m}^2 \text{ g}^{-1}$  before calcination; however, after calcination, the specific surface area decreased to about  $50 \text{ m}^2 \text{ g}^{-1}$ . Thermally stable and large-pore mesoporous titania with low structural regularity were obtained in a synthesis by combining amphiphilic poly(alkylene oxide) block copolymers as structure-directing agents and inorganic titanium salts in a non-aqueous (ethanol) solution.<sup>[123]</sup>

The miniemulsion process was shown to be a very suitable technique that enables the transformation of monodisperse stable droplets into  $\text{TiO}_2$  nanoparticles. During hydrolysis and condensation, each droplet acts as a nanoreactor under preservation of droplet size, droplet number, and the concentration in each droplet.<sup>[124]</sup> Recently, Zhang et al.<sup>[125]</sup> reported a synthesis of solid anatase nanoparticles of about 15 nm in size and with a specific surface area of  $170 \text{ m}^2 \text{ g}^{-1}$  by applying the inverse miniemulsion technique with tetrabutyltitanate as precursor. The as-synthesized particles are amorphous, and phase transition to anatase is only induced after thermal treatment at  $550^\circ\text{C}$ , which is probably a consequence of the fast condensation reaction of the precursor material.

A combination of sol-gel processing of bis(2-hydroxyethyl)titanate (EGMT) as precursor with the inverse miniemulsion technique led to a novel template-free approach to synthesize spherical porous anatase particles at a reaction temperature of  $100^\circ\text{C}$  and with an average size of about 200 nm (Figure 19).<sup>[124]</sup> The only surfactant employed was the

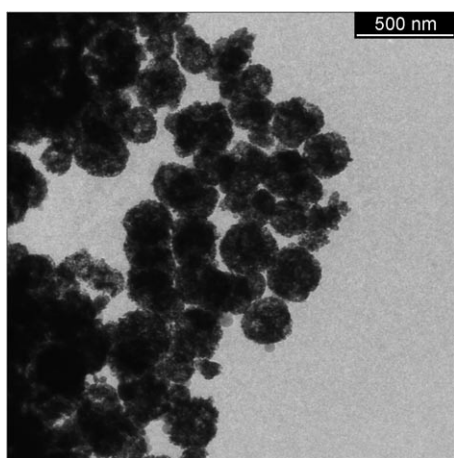


**Figure 19.** TEM image of mesoporous  $\text{TiO}_2$  (anatase) nanoparticles prepared by the miniemulsion process.

block copolymer poly(E/B-*block*-EO) (EO = ethylene oxide, B = butylene), which stabilizes the aqueous droplets with the water-soluble precursor bis(2-hydroxyethyl)titanate (EGMT) in the organic phase, but also leads to aggregation and pore formation inside the particles. The lower relative rates of hydrolysis and condensation compared to the commonly used titanium alkoxides allow convenient handling in the miniemulsion. The crystalline phase composition inside the nano-

particles could be easily adjusted by changing the synthesis temperature, varying the ratio of precursor to hydrochloric acid, and by using a mixture of hydrochloric acid and ethylene glycol as the dispersed phase. To obtain pure anatase, a temperature of  $100^\circ\text{C}$  and a molar ratio of precursor to hydrochloric acid of 1:5.4 has to be employed, leading to a specific surface area as high as  $140 \text{ m}^2 \text{ g}^{-1}$ . With a volume ratio of hydrochloric acid to ethylene glycol of 1:4 as dispersed phase, a complete preservation of the spherical aggregation could be obtained after calcination at  $400^\circ\text{C}$  and with a specific surface area of about  $120 \text{ m}^2 \text{ g}^{-1}$ . The crystallite size and therefore the specific surface area can be easily adjusted by the amount of surfactant poly(E/B-*block*-ethylene oxide) that is responsible for stabilizing the inverse miniemulsion. With 5 wt % of surfactant with respect to the dispersed phase, the specific surface area could be increased to a value higher than  $300 \text{ m}^2 \text{ g}^{-1}$ .

The advantage of this new synthetic approach is the ability to produce selectively anatase nanocrystals arranged in a spherical manner without any calcination step. Thus, no thermal treatment for crystallization is necessary. Even after calcination at  $400^\circ\text{C}$  for complete removal of the surfactant, a high specific surface area of more than  $300 \text{ m}^2 \text{ g}^{-1}$  can be preserved. This result is of interest for catalyst supports, sorption media, and in particular in photocatalysis, because the photocatalytic activity increases with increasing specific surface area.

In a different approach, crystalline inorganic materials were obtained by using cross-linked gelatin nanoparticles, which were synthesized by the inverse miniemulsion process<sup>[126]</sup> as nanoenvironment and template for crystal growth in the aqueous phase.<sup>[127]</sup> The synthesis of gelatin nanoparticles using the inverse miniemulsion technique is itself intriguing owing to the flexibility offered by the technique in tailoring the properties of the gelatin nanoparticles. The nanoenvironment promotes a different growth environment for the crystal because of the confinement inside the particle. The formation of hydroxyapatite (Figure 20) inside the particles follows Ostwald's rule of stages. An amorphous phase is initially formed, which has great potential in itself to be used as a resorbable bone substitute. This phase further transforms into single-crystalline hydroxyapatite via an octacalcium phosphate intermediate.

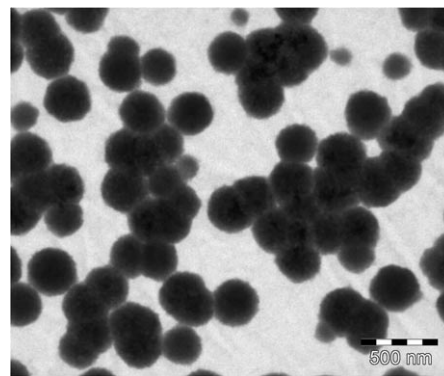


**Figure 20.** TEM image of hybrid gelatine/hydroxyapatite nanoparticles.



Other conceptual approaches in which hybrid calcium phosphate nanoparticles were synthesized by employing organic additives or templates, such as surfactants,<sup>[128–130]</sup> liposomes,<sup>[131,132]</sup> block copolymers,<sup>[133,134]</sup> self-associated nanogels,<sup>[135]</sup> supramolecular hydrogels,<sup>[136]</sup> emulsions, and microemulsions,<sup>[137–139]</sup> have also been reported. Owing to the feasibility of controlling shape, size, crystal structure, and orientation, the organization of inorganic colloids in polymeric matrices has led to biomimetic approaches being intensively explored. The matrix mediation and the molecular templating for mineralization have shed light on the interfacial chemistry between the organic and inorganic components and also the mechanisms of crystallization in association with the coreactants.<sup>[140,141]</sup> Extensive studies on organized assemblies of amphiphilic molecules have shown them to provide a suitable environment for the synthesis of controlled nanoscale assemblies of biologically relevant inorganic materials. Mesoscale transformations lead to the involvement of cooperative reorganization of inorganic and organic building blocks and the emergence of higher order complex architectures.<sup>[142–144]</sup>

### 9. Crystallization in Nanoparticles

The undercooling required to obtain crystallization in miniemulsion droplets is significantly increased compared to the bulk material; for hexadecane droplets, a shift from 12 °C (bulk) to about –4 °C (droplets), for the NaCl solution a shift from –22 °C (bulk) to –46 °C (droplets) (Figure 21),<sup>[145]</sup> and

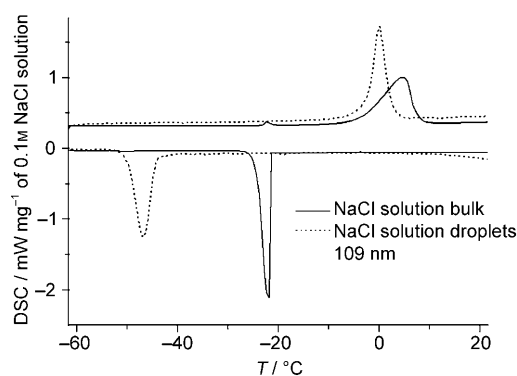


**Figure 21.** Comparison of sodium chloride solution in bulk (0.1 M) and in the inverse miniemulsion with differential scanning calorimetry (DSC). Cooling (lower curve) and heating rates (upper): 5 K min<sup>-1</sup>.

for poly(ethylene glycol) a shift from 43 °C (bulk) to about –23 °C (droplets)<sup>[146]</sup> is observed. These results can be explained by the fact that in miniemulsions, each droplet has to be nucleated separately, and the nucleation mechanism is shifted from heterogeneous to homogeneous nucleation. Furthermore, the undercooling increases with decreasing temperature, which is explained by finite size effects for spinodal (spontaneous) decompositions. The interfacial tension does not have any influence on the crystallization process. The crystallization rate in miniemulsion droplets is

higher than that of the bulk and is proportional to the droplet size.

An interesting behavior was detected for odd- and even-chain-length alkanes.<sup>[147]</sup> In even alkanes, the confinement in small droplets changes the bulk crystal structure from triclinic to orthorhombic, which is attributed to finite size effects inside the droplets. During cooling, an intermediate rotator phase (metastable phase) is not detected for the miniemulsion droplets. As the nucleation barrier causes crystallization well below the equilibrium melting point, at the temperature of observed crystallization, the equilibrium structure is crystalline. On (equilibrium) heating, the transition into a rotator phase is detected. For odd alkanes, only a strong crystallization temperature shift relative to the bulk system but no structure change is observed, as both in bulk and in miniemulsion droplets, an orthorhombic structure is formed.

Inside crystallizing PEG droplets, four to five lamellae are formed that are not interlamellar-connected, but rather simply loosely layered.<sup>[146]</sup> During crystallization, only one nucleus is present in each droplet at one time. Upon large supercooling, only about 60 % of the chains are crystallized, indicating a high imperfection of the superstructure. However, a rearrangement occurs at increasing temperature. Whereas in dispersion the structure is stable, upon drying, the lamellae slide apart from each other and arrange in a highly ordered, xenon-structural fashion (see pattern in Figure 22). The smallest units (the “cap” of the droplet) consists of as little as one polymer chain. Therefore, the crystallization of polymers confined in miniemulsions can also be used to obtain single-chain single crystals.

Different preformed smectic polysiloxanes have been used for the formulation of miniemulsions with droplet sizes of between 100 and 300 nm. Smectic layers within the droplet could be detected by electron microscopy.<sup>[148]</sup>

A structuring of liquid crystal (E7) nanodroplets, with droplet sizes between 180 and 630 nm, was also successfully prepared by the miniemulsion approach.<sup>[149]</sup> DSC measurements showed that the nematic–isotropic temperature of the droplets is 41 °C, which is much lower than that of the bulk (59 °C). From AFM analysis, some forms of imperfect smectic

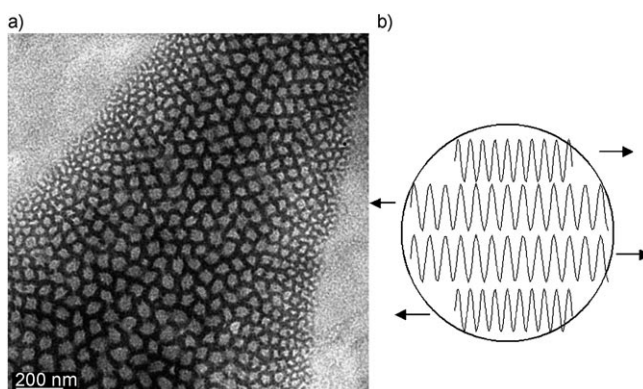


**Figure 22.** a) Electron micrograph obtained of the inverse miniemulsion with poly(ethylene oxide) (PEO;  $M_w = 12\,000\text{ g mol}^{-1}$ ). b) Representation of the loosely packed PEO lamellae in the droplets; the lamellae can slide apart during drying.

molecular arrangement were formed because of the order of the liquid crystal droplets (Figure 23). The light-scattering results confirm that the liquid crystal droplets prepared by the

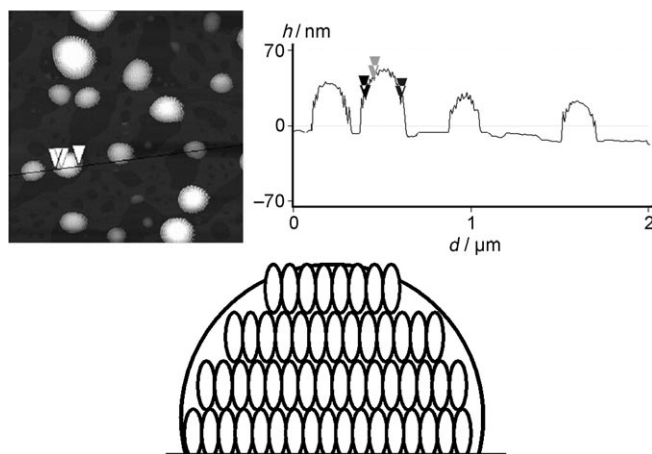


**Figure 23.** Top right: Representative section analysis of liquid crystal miniemulsion droplets, showing the “hedgehog” structures along the line in the AFM image (top left). The horizontal distances between the peaks are constant at 7.813 nm; vertical distances: 17.355 nm, 11.514 nm, and 9.790 nm. Bottom: Representation of the liquid crystal molecular arrangement in a droplet.

miniemulsion approach are stable over a period of time even when heating and cooling steps and those droplets are anisotropic. The anisotropy of liquid crystal droplets diminishes drastically (approximately between the temperatures of 43–48 °C) on heating and cooling, which is in good agreement with nematic–isotropic temperature measured by the DSC experiment. The remaining small fraction of anisotropy is attributed to a thin nematic interface layer, which is similar to orientational wetting of planar interfaces above the nematic–isotropic phase-transition temperature. The depolarized dynamic light scattering gives access to internal fluctuation modes of the liquid-crystalline droplets.

The crystallization of the miniemulsions of dyes with primary droplet diameters of 120 nm was shown to result in single-crystalline nanofibers of high quality, uniformity, and chromatic definition (Figure 24).<sup>[150]</sup> As these dyes are absolutely insoluble in the continuous phase, the observed growth of the crystals must have proceeded by controlled aggregation and mesoscale transformation of colloidal intermediates. This case can be regarded as a model for this nonclassical

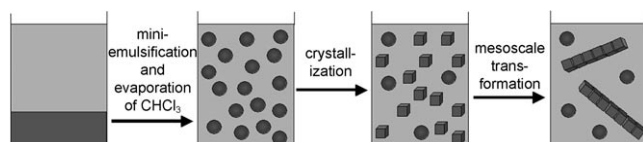


**Figure 24.** Preparation of a dye miniemulsion resulting in 100 nm separated compartments (step 1). The single droplets can undergo crystallization (step 2), and in case of insufficient colloidal stability of the nanocrystals, a mesoscale transformation (step 3).

crystallization process, which has been postulated to explain many morphosynthesis experiments of inorganic species by a variety of research groups, but not elaborated in the clarity possible for this system.

The fact that the crystals of those dyes are pleochromic reveals additional information about the aggregation process. Dye absorption, and therefore the maximum dipole moment, are oriented perpendicular to the growth direction, which gives strong indications that the controlled aggregation is mediated not by dipole fields (as usually speculated), but by polarization forces. As these fields add up coherently for polar crystals in a highly anisotropic fashion, van der Waals attraction in certain direction can obviously become very strong, and indeed much stronger than the ionic and steric stabilizers that keep the original miniemulsion stable. This effect can be called a “super van der Waals” force, which is highly directional and breaks the radial symmetry of the DLVO potential (DLVO: Derjaguin, Landau, Verwey, Overbeek). As a result, highly selective and spatially controlled aggregation takes place, which is the prerequisite of morphosynthetic control of the crystal habit.

The existence of such forces also explain why industrially optimized procedures to make dye or drug nanocrystals<sup>[151]</sup> succeed or fail from system to system in a way that is not predictable from the properties of the molecule alone. According to the model described above, stable nanocrystals can only be made from crystal structures that do not show coherent addition of molecular polarizabilities.

## 10. Structuring with Nanoparticles

Highly monodisperse metal-containing nanoparticles could also be used for nanolithography (Figure 25). This novel approach to prepare highly ordered arrays of silicon nanopillars or nanoholes that both exhibit aspect ratios of up to ten is again based on the miniemulsion technique, enabling the fabrication of spherical colloidal particles loaded with a platinum complex (see Section 3.1). These particles are used as carriers during their self-assembly into hexagonally ordered arrays on top of silicon substrates.<sup>[152]</sup> The colloids can be loaded with virtually any precursor material, which makes the miniemulsion technique promising for many different metals. Though the additionally applied etching processes are similar to those previously developed for micellar particles,<sup>[153]</sup> it was by no means obvious that these procedures will conserve the original hexagonal order of the colloids. The experimental evidence provided by the arrays of silicon nanopillars and holes allows the exploitation of still another strength of the present approach; that is, to realize interparticle distances well beyond those obtainable by the micellar method.<sup>[154]</sup>

Stable precursor nanoparticles of complex lanthanide phosphors with binary and ternary composition as obtained in the inverse miniemulsion process can be used to for inorganic crystalline films that can be very thin and highly homogeneous in topography and structure (Figure 26).<sup>[155]</sup> In a subsequent annealing process, the precursor materials are converted into films of red, green, or blue phosphor. In the

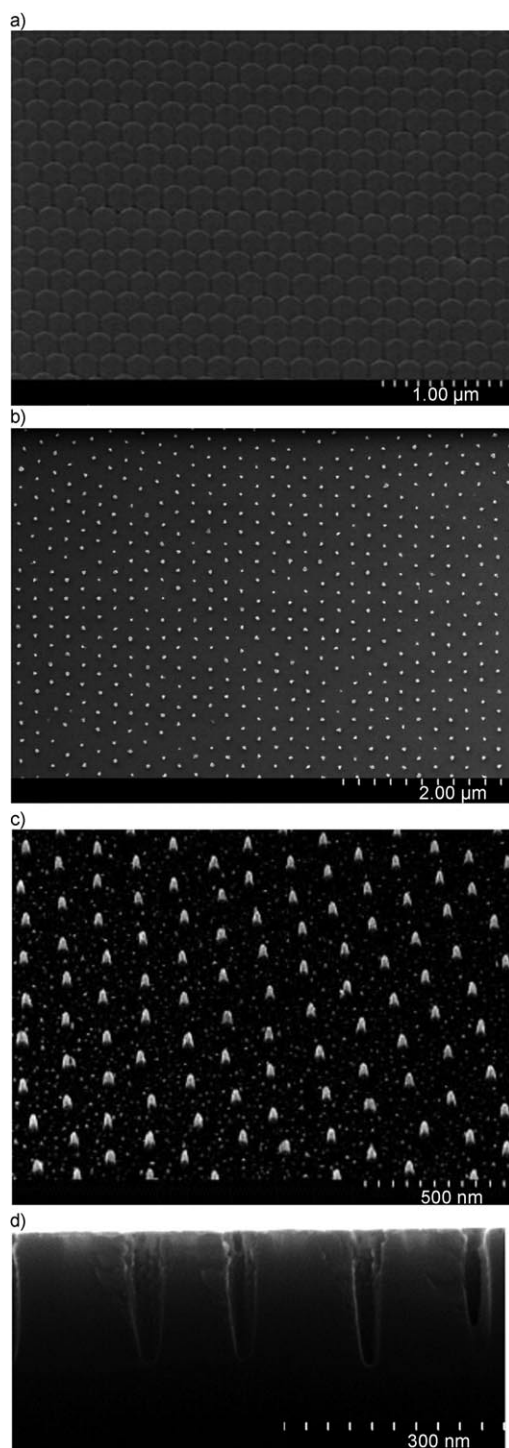


**Figure 25.** a,b) SEM images showing films of monodisperse platinum-containing polymer particles a) before and b) after plasma etching. The particles used as templates c) for columns or d) holes with a depth of 180 nm.

case of the red phosphor, “single-crystal films” are formed that show a surface roughness in the order of single-crystalline surfaces.

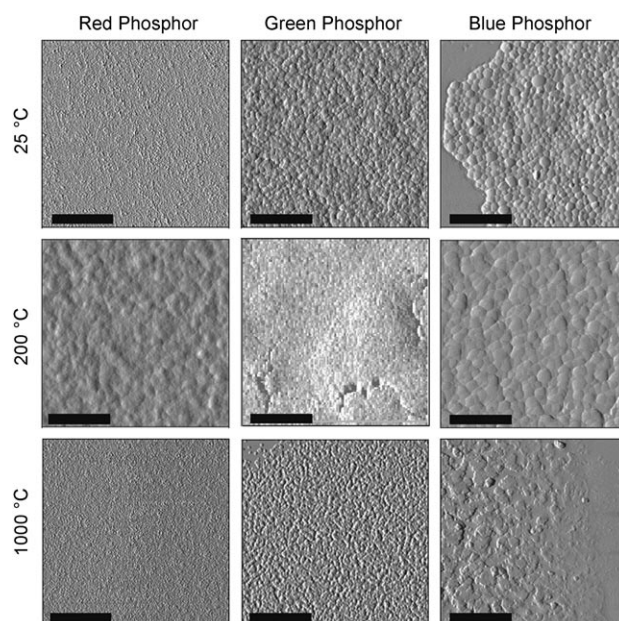


**Figure 26.** AFM amplitude pictures of red, green, and blue phosphor films at room temperature and after annealing at 200 °C and 1000 °C; red:  $\text{Y}_{0.94}\text{Eu}_{0.06}\text{O}_3$ , green:  $\text{La}_{0.5}\text{Ce}_{0.3}\text{Tb}_{0.2}\text{PO}_4$ , blue:  $\text{Ba}_{0.9}\text{Eu}_{0.1}\text{MgAl}_{10}\text{O}_{17}$ . The bar corresponds to 1 μm.

## 11. Conclusion

The miniemulsion process is a versatile technique for the formation of nanoparticles obtained by different polymerization methods, ranging from radical, anionic, cationic, and enzymatic polymerization to polycondensation and polyaddition. A surface functionalization of the nanoparticles can be obtained by copolymerization reactions. It could be demonstrated that the miniemulsion process is well-suited for the encapsulation of various materials: hydrophobic or hydrophobized solids can be encapsulated in hydrophobic polymers, and hydrophilic or hydrophobic liquids can be used for the formation of nanocapsules in inverse or direct miniemulsion emulsions. For the nanoparticle formation, different procedures are described in the literature: a phase separation mechanism, an interfacial reaction at the nanodroplet interface, and a nanoprecipitation of the polymer onto the nanodroplets. The release of the components can be tuned to be effective for a long time period or suddenly after applying a stimulus. The morphology of polymer–polymer nanoparticles was shown to be dictated by the compatibility of the polymers and the surface tensions of the different interfaces. The nanodroplets can also be used for crystallization or polymeric nanoparticles as templates for crystallization. A suppression of the crystallization allowed the formation of very thin and homogeneous crystalline films, and homogeneous metal-loaded nanoparticles were used for novel nanolithography. The examples in the review show the broad possibility of the miniemulsion process, opening the possibility to many more developments in the future.

Received: February 6, 2009

Published online: May 19, 2009



- [1] K. Landfester, *Annu. Rev. Mater. Res.* **2006**, *36*, 231.
- [2] J. M. Asua, *Prog. Polym. Sci.* **2002**, *27*, 1283.
- [3] F. J. Schork, Y. W. Luo, W. Smulders, J. P. Russum, A. Butte, K. Fontenot, *Adv. Polym. Sci.* **2005**, *175*, 129.
- [4] D. Crespy, K. Landfester, *Macromolecules* **2005**, *38*, 6882.
- [5] C. K. Weiss, U. Ziener, K. Landfester, *Macromolecules* **2007**, *40*, 928.
- [6] S. Cauvin, F. Ganachaud, *Macromol. Symp.* **2004**, *215*, 179.
- [7] S. Cauvin, F. Ganachaud, M. Moreau, P. Hemery, *Chem. Commun.* **2005**, 2713.
- [8] R. Soula, B. Saillard, R. Spitz, J. Claverie, M. F. Llauro, C. Monnet, *Macromolecules* **2002**, *35*, 1513.
- [9] P. Wehrmann, M. Zuideveld, R. Thomann, S. Mecking, *Macromolecules* **2006**, *39*, 5995.
- [10] A. Held, I. Kolb, M. A. Zuideveld, R. Thomann, Stefan Mecking, M. Schmid, R. Pietruschka, E. Lindner, M. Khanfar, M. Sunjuk, *Macromolecules* **2002**, *35*, 3342.
- [11] D. Quémener, V. Héroguez, Y. Gnanou, *Macromolecules* **2005**, *38*, 7977.
- [12] D. Quémener, V. Héroguez, Y. Gnanou, *J. Polym. Sci. Part A* **2006**, *44*, 2784.
- [13] P. Wehrmann, S. Mecking, *Macromolecules* **2006**, *39*, 5963.
- [14] J. Huber, S. Mecking, *Polym. Mater. Sci. Eng.* **2007**, *96*, 306.
- [15] J. Pecher, S. Mecking, *Macromolecules* **2007**, *40*, 7733.
- [16] K. Landfester, F. Tiarks, H.-P. Hentze, M. Antonietti, *Macromol. Chem. Phys.* **2000**, *201*, 1.
- [17] F. Tiarks, K. Landfester, M. Antonietti, *J. Polym. Sci. Polym. Chem. Ed.* **2001**, *39*, 2520.
- [18] M. Barrère, K. Landfester, *Macromolecules* **2003**, *36*, 5119.
- [19] M. Baile, Y. J. Chou, J. C. Saam, *Polym. Bull.* **1990**, *23*, 251.
- [20] J. C. Saam, Y. J. Chou, US Patent 4355154, **1982**.
- [21] M. Barrère, K. Landfester, *Polymer* **2003**, *44*, 2833.
- [22] S. Kobayashi, H. Uyama, S. Suda, S. Namekawa, *Chem. Lett.* **1997**, 105.
- [23] H. Uyama, K. Inada, S. Kobayashi, *Chem. Lett.* **1998**, 1285.
- [24] S. Namekawa, H. Uyama, S. Kobayashi, *Polym. J.* **1998**, *30*, 269.
- [25] A. Taden, M. Antonietti, K. Landfester, *Macromol. Rapid Commun.* **2003**, *24*, 512.
- [26] A. Musyanovych, V. Mailänder, K. Landfester, *Biomacromolecules* **2005**, *6*, 1824.
- [27] E. Marie, R. Rothe, M. Antonietti, K. Landfester, *Macromolecules* **2003**, *36*, 3967.
- [28] S. Bhadra, N. K. Singha, D. Khastgir, *Synth. Met.* **2006**, *156*, 1148.
- [29] F. M. Bauers, S. Mecking, *Angew. Chem.* **2001**, *113*, 3112; *Angew. Chem. Int. Ed.* **2001**, *40*, 3020.
- [30] R. Soula, C. Novat, A. Tomov, R. Spitz, J. Claverie, X. Drujon, J. Malinge, T. Saudemont, *Macromolecules* **2001**, *34*, 2022.
- [31] F. M. Bauers, R. Thomann, S. Mecking, *J. Am. Chem. Soc.* **2003**, *125*, 8838.
- [32] V. Monteil, A. Bastero, S. Mecking, *Macromolecules* **2005**, *38*, 5393.
- [33] J. Huber, S. Mecking, *Angew. Chem.* **2006**, *118*, 6462; *Angew. Chem. Int. Ed.* **2006**, *45*, 6314.
- [34] K. Landfester, R. Montenegro, U. Scherf, R. Güntner, U. Asawapirom, S. Patil, T. Kietzke, D. Neher, *Adv. Mater.* **2002**, *14*, 651.
- [35] A. Musyanovych, J. Schmitz-Wienke, V. Mailänder, P. Walther, K. Landfester, *Macromol. Biosci.* **2008**, *8*, 127.
- [36] D. L. Tillier, J. Meuldijk, C. E. Koning, *Polymer* **2003**, *44*, 7883.
- [37] E. Schreiber, U. Ziener, A. Manske, A. Plettl, P. Ziemann, K. Landfester, *Chem. Mater.* **2009**, *21*, 1750.
- [38] L. Ramírez, M. Antonietti, K. Landfester, *Macromol. Chem. Phys.* **2006**, *207*, 160.
- [39] V. Holzapfel, A. Musyanovych, K. Landfester, M. R. Lorenz, V. Mailänder, *Macromol. Chem. Phys.* **2005**, *206*, 2440.
- [40] J.-L. Luna-Xavier, A. Guyot, E. Bourgeat-Lami, *J. Colloid Interface Sci.* **2002**, *250*, 82.
- [41] P. Espiard, A. Guyot, *Polymer* **1995**, *36*, 4391.
- [42] Y. Haga, T. Watanabe, R. Yosomiya, *Angew. Makromol. Chem.* **1991**, *189*, 23.
- [43] L. Quaroni, G. Chumanov, *J. Am. Chem. Soc.* **1999**, *121*, 10642.
- [44] E. Bourgeat-Lami, J. Lang, *J. Colloid Interface Sci.* **1998**, *197*, 293.
- [45] E. Bourgeat-Lami, J. Lang, *J. Colloid Interface Sci.* **1999**, *210*, 281.
- [46] E. Bourgeat-Lami, J. Lang, *Macromol. Symp.* **2000**, *151*, 377.
- [47] I. Sondi, T. H. Fedynshyn, R. Sinta, E. Matijević, *Langmuir* **2000**, *16*, 9031.
- [48] K. Landfester, N. Bechthold, S. Förster, M. Antonietti, *Macromol. Rapid Commun.* **1999**, *20*, 81.
- [49] S. Lelu, C. Novat, C. Graillat, A. Guyot, E. Bourgeat-Lami, *Polym. Int.* **2003**, *52*, 542.
- [50] N. Bechthold, F. Tiarks, M. Willert, K. Landfester, M. Antonietti, *Macromol. Symp.* **2000**, *151*, 549.
- [51] B. Erdem, E. D. Sudol, V. L. Dimonie, M. S. El-Aasser, *J. Polym. Sci. Part A* **2000**, *38*, 4419; B. Erdem, E. D. Sudol, V. L. Dimonie, M. S. El-Aasser, *J. Polym. Sci. Part A* **2000**, *38*, 4431; B. Erdem, E. D. Sudol, V. L. Dimonie, M. S. El-Aasser, *J. Polym. Sci. Part A* **2000**, *38*, 4441.
- [52] G. H. Al-Ghamdi, E. D. Sudol, V. L. Dimonie, M. S. El-Aasser, *J. Appl. Polym. Sci.* **2006**, *101*, 3479.
- [53] D. Hoffmann, K. Landfester, M. Antonietti, *Magnetohydrodynamics* **2001**, *37*, 217.
- [54] F. Fleischhaker, R. Zentel, *Chem. Mater.* **2005**, *17*, 1346.
- [55] A. C. C. Esteves, L. Bombalski, T. Trindade, K. Matyjaszewski, A. Barros-Timmons, *Small* **2007**, *3*, 1230.
- [56] Y. Gao, S. Reischmann, J. Huber, T. Hanke, R. Bratschitsch, A. Leitenstorfer, S. Mecking, *Colloid Polym. Sci.* **2008**, *286*, 1329.
- [57] R. Bouanani, D. Bendedouch, P. Hemery, B. Bounaceur, *Colloids Surf. A* **2008**, *317*, 751.
- [58] G. Diaconu, M. Paulis, J. R. Leiza, *Macromol. React. Eng.* **2008**, *2*, 80.
- [59] F. Tiarks, K. Landfester, M. Antonietti, *Langmuir* **2001**, *17*, 5775.
- [60] V. Monteil, J. Stumbaum, R. Thomann, Stefan Mecking, *Macromolecules* **2006**, *39*, 2056.
- [61] E. I. López-Martínez, A. Marquez-Lucero, C. A. Hernandez-Escobar, S. G. Flores-Gallardo, R. Ibarra-Gomez, M. J. Yacamán, E. A. Zaragoza-Contreras, *J. Polym. Sci. Part B* **2007**, *45*, 511.
- [62] H. Kim, E. S. Daniels, S. Li, V. K. Makkapati, K. Kardos, *J. Polym. Sci. Part A* **2007**, *45*, 1038.
- [63] B. Bailly, A. C. Donnenwirth, C. Bartholome, E. Beyou, E. Bourgeat-Lami, *J. Nanomater.* **2006**, DOI: 10.1155/JNM/2006/76371.
- [64] F. Tiarks, K. Landfester, M. Antonietti, *Macromol. Chem. Phys.* **2001**, *202*, 51.
- [65] N. Steiert, K. Landfester, *Macromol. Mater. Eng.* **2007**, *292*, 1111.
- [66] L. P. Ramirez, K. Landfester, *Macromol. Chem. Phys.* **2003**, *204*, 22.
- [67] V. Holzapfel, M. R. Lorenz, C. K. Weiss, H. Schrezenmeier, K. Landfester, V. Mailänder, *J. Phys. Condens. Matter* **2006**, *18*, 2581.
- [68] G. E. Hildebrand, J. W. Tack, *Int. J. Pharm.* **2000**, *196*, 173.
- [69] U. Bilati, E. Allemann, E. Doelker, *AAPS PharmSciTech* **2005**, *6*, E594.
- [70] B. R. Conway, H. Oya Alpar, *Eur. J. Pharm. Biopharm.* **1996**, *42*, 42.
- [71] D. Quintanar-Guerrero, E. Allemann, E. Doelker, H. Fessi, *Pharm. Res.* **1998**, *15*, 1056.

- [72] C. X. Song, V. Labhasetwar, H. Murphy, X. Qu, W. R. Humphrey, R. J. Shebuski, R. J. Levy, *J. Controlled Release* **1997**, *43*, 197.
- [73] S. Hariharan, V. Bhardwaj, I. Bala, J. Sitterberg, U. Bakowsky, M. N. V. Ravi Kumar, *Pharm. Res.* **2006**, *23*, 184.
- [74] E. Allémann, J. C. Leroux, R. Gurny, E. Doelker, *Pharm. Res.* **1993**, *10*, 1732.
- [75] A. P. R. Johnston, C. Cortez, A. S. Angelatos, F. Caruso, *Curr. Opin. Colloid Interface Sci.* **2006**, *11*, 203.
- [76] N. Kato, P. Schuetz, F. Caruso, *Macromolecules* **2002**, *35*, 9780.
- [77] W. J. Tong, C. Y. Gao, H. Mohwald, *Polym. Adv. Technol.* **2008**, *19*, 817.
- [78] C. J. Ochs, G. K. Such, B. Stadler, F. Caruso, *Biomacromolecules* **2008**, *9*, 3389.
- [79] F. Tiarks, K. Landfester, M. Antonietti, *Langmuir* **2001**, *17*, 908.
- [80] M. Volz, U. Ziener, U. Salz, J. Zimmermann, K. Landfester, *Colloid Polym. Sci.* **2007**, *285*, 687.
- [81] S. Theisinger, K. Schoeller, B. Osborn, M. Sarkar, K. Landfester, *Macromol. Chem. Phys.* **2009**, *210*, 411.
- [82] Y. W. Luo, H. Y. Gu, *Polymer* **2007**, *48*, 3262.
- [83] D. Crespy, M. Stark, C. Hoffmann-Richter, U. Ziener, K. Landfester, *Macromolecules* **2007**, *40*, 3122.
- [84] R. Arshady, *J. Microencapsulation* **1989**, *6*, 13.
- [85] L. Danicher, Y. Frere, A. Le Calve, *Macromol. Symp.* **2000**, *151*, 387.
- [86] L. Torini, J. F. Argillier, N. Zydowicz, *Macromolecules* **2005**, *38*, 3225.
- [87] C. Scott, D. Wu, C.-C. Ho, C. C. Co, *J. Am. Chem. Soc.* **2005**, *127*, 4160.
- [88] D. Sarkar, J. El-Khoury, S. T. Lopina, J. Hu, *Macromolecules* **2005**, *38*, 8603.
- [89] E. Allémann, J.-C. Leroux, R. Gurny, *Adv. Drug Delivery Rev.* **1998**, *34*, 171.
- [90] C. Vauthier, C. Dubernet, E. Fattal, H. Pinto-Alphandary, P. Couvreur, *Adv. Drug Delivery Rev.* **2003**, *55*, 519.
- [91] D. Crespy, K. Landfester, *Macromol. Chem. Phys.* **2007**, *208*, 457.
- [92] E. Marie, K. Landfester, M. Antonietti, *Biomacromolecules* **2002**, *3*, 475.
- [93] N. Jagielski, S. Sharma, V. Hombach, V. Mailänder, V. Rasche, K. Landfester, *Macromol. Chem. Phys.* **2007**, *208*, 2229.
- [94] D. Wu, C. Scott, C. C. Ho, C. C. Co, *Macromolecules* **2006**, *39*, 5848.
- [95] A. Musyanovych, K. Landfester, *Prog. Colloid Polym. Sci.* **2008**, *134*, 120.
- [96] T. J. De Faria, A. M. De Campos, E. L. Senna, *Macromol. Symp.* **2005**, *229*, 228.
- [97] U. Paiphansiri, P. Tangboriboonrat, K. Landfester, *Macromol. Biosci.* **2006**, *6*, 33.
- [98] B. zu Putlitz, K. Landfester, H. Fischer, M. Antonietti, *Adv. Mater.* **2001**, *13*, 500.
- [99] T. Kietzke, D. Neher, M. Kumke, O. Ghazy, U. Ziener, K. Landfester, *Small* **2007**, *3*, 1041.
- [100] T. Kietzke, D. Neher, K. Landfester, R. Montenegro, R. Güntner, U. Scherf, *Nat. Mater.* **2003**, *2*, 408.
- [101] T. Kietzke, D. Neher, M. Kumke, R. Montenegro, K. Landfester, U. Scherf, *Macromolecules* **2004**, *37*, 4882.
- [102] A. Guyot, K. Landfester, J. P. Schork, Ch. Wang, *Prog. Polym. Sci.* **2007**, *32*, 1439.
- [103] S. T. Wang, F. J. Schork, G. W. Poehlein, J. W. Gooch, *J. Appl. Polym. Sci.* **1996**, *60*, 2069.
- [104] X. Wu, F. Schork, J. Gooch, *J. Polym. Sci. Polym. Chem.* **1999**, *37*, 4159.
- [105] J. Tsavalas, Y. Luo, L. Hudda, F. Schork, *Polym. React. Eng.* **2003**, *11*, 277.
- [106] J. Tsavalas, F. Schork, K. Landfester, *J. Res.* **2004**, *1*, 53.
- [107] J. Tsavalas, J. Gooch, F. Schork, *J. Appl. Polym. Sci.* **2000**, *75*, 916.
- [108] J. Gooch, H. Dong, F. Schork, *J. Appl. Polym. Sci.* **2000**, *76*, 105.
- [109] M. Li, E. Daniels, V. Dimonie, E. Sudol, M. El-Aasser, *Macromolecules* **2005**, *38*, 4183.
- [110] C. Wang, F. Chu, C. Graillat, A. Guyot, C. Gauthier, J. P. Chapel, *Polymer* **2005**, *46*, 1113.
- [111] J. Guo, F. J. Schork, *Macromol. React. Eng.* **2008**, *2*, 265.
- [112] K. Landfester, R. Rothe, M. Antonietti, *Macromolecules* **2002**, *35*, 1658.
- [113] M. Barrère, K. Landfester, *Macromolecules* **2003**, *36*, 5119.
- [114] K. Landfester, U. Pawelzik, M. Antonietti, *Polymer* **2005**, *46*, 9892.
- [115] A. Koenig, U. Ziener, A. Schaz, K. Landfester, *Macromol. Chem. Phys.* **2007**, *208*, 155.
- [116] C. K. Weiss, M. R. Lorenz, K. Landfester, V. Mailänder, *Macromol. Biosci.* **2007**, *7*, 883.
- [117] C. Weiss, M. V. Kohnle, K. Landfester, T. Hauk, D. Fischer, J. Schmitz-Wienke, V. Mailänder, *ChemMedChem* **2008**, *3*, 1395.
- [118] U. Paiphansiri, J. Dausend, A. Musyanovych, V. Mailänder, K. Landfester, *Macromol. Biosci.*, DOI: 10.1002/mabi.200800293.
- [119] M. Volz, P. Walther, U. Ziener, K. Landfester, *Macromol. Mater. Eng.* **2007**, *292*, 1237.
- [120] H. Shibata, T. Ogura, T. Mukai, T. Ohkubo, H. Sakai, M. Abe, *J. Am. Chem. Soc.* **2005**, *127*, 16396; H. Shibata, H. Mihara, T. Mukai, T. Ogura, H. Kohno, T. Ohkubo, H. Sakai, M. Abe, *Chem. Mater.* **2006**, *18*, 2256; A. Testino, I. R. Bellobono, V. Buscaglia, C. Canevali, M. D'Arienzo, S. Polizzi, R. Scotti, F. Morazzoni, *J. Am. Chem. Soc.* **2007**, *129*, 3564; J. Xu, L. Liping, Y. Yan, H. Wang, X. Wang, X. Fu, G. Li, *J. Colloid Interface Sci.* **2008**, *318*, 29; S. Mahshid, M. Askari, M. S. Ghamsari, *Int. J. Mater. Prod. Technol.* **2007**, *189*, 296; H. Liu, W. Yang, Y. Ma, Y. Cao, J. Yao, J. Zhang, T. Hu, *Langmuir* **2003**, *19*, 3001; H. Zhang, J. F. Banfield, *Chem. Mater.* **2002**, *14*, 4145; B. A. Morales, O. Novaro, T. López, E. Sánchez, R. Gómez, *Mater. Res. Soc. Symp. Proc.* **1995**, *10*, 2788; E. Matijevic, M. Budnik, L. Meites, *J. Colloid Interface Sci.* **1977**, *61*, 302.
- [121] D. M. Antonelli, J. Y. Ying, *Angew. Chem.* **1995**, *107*, 2202; *Angew. Chem. Int. Ed. Engl.* **1995**, *34*, 2014.
- [122] D. M. Antonelli, *Microporous Mesoporous Mater.* **1999**, *30*, 315.
- [123] P. Yang, D. Zhao, D. I. Margolese, B. F. Chmelka, G. D. Stucky, *Nature* **1998**, *396*, 152.
- [124] R. Rossmanith, C. K. Weiss, J. Geserick, N. Huesing, U. Hörmann, K. Landfester, *Chem. Mater.* **2008**, *20*, 5768.
- [125] S. Zhang, Q. Yu, Z. Chen, Y. Li, Y. You, *Mater. Lett.* **2007**, *61*, 4839.
- [126] A. Ethirajan, K. Schoeller, A. Musyanovych, U. Ziener, K. Landfester, *Biomacromolecules* **2008**, *9*, 2383.
- [127] A. Ethirajan, U. Ziener, A. Chuvilin, U. Kaiser, H. Cölfen, K. Landfester, *Adv. Funct. Mater.* **2008**, *18*, 2221.
- [128] T. Welzel, W. Meyer-Zaika, M. Eppele, *Chem. Commun.* **2004**, 1204.
- [129] C. E. Fowler, M. Li, S. Mann, H. C. Margolis, *J. Mater. Chem.* **2005**, *15*, 3317.
- [130] S. Sarda, M. Heughebaert, A. Lebugle, *Chem. Mater.* **1999**, *11*, 2722.
- [131] H. T. Schmidt, A. E. Ostafin, *Adv. Mater.* **2002**, *14*, 532.
- [132] H. T. Schmidt, B. L. Gray, P. A. Wingert, A. E. Ostafin, *Chem. Mater.* **2004**, *16*, 4942.
- [133] M. Antonietti, M. Breulmann, C. G. Göltner, H. Cölfen, K. K. W. Wong, D. Walsh, S. Mann, *Chem. Eur. J.* **1998**, *4*, 2493.
- [134] Y. Kakizawa, K. Miyata, S. Furukawa, K. Kataoka, *Adv. Mater.* **2004**, *16*, 699.
- [135] A. Sugawara, S. Yamane, K. Akiyoshi, *Macromol. Rapid Commun.* **2006**, *27*, 441.
- [136] Z. A. C. Schnepp, R. Gonzalez-McQuire, S. Mann, *Adv. Mater.* **2006**, *18*, 1869.

- [137] G. K. Lim, J. Wang, S. C. Ng, L. M. Gan, *Langmuir* **1999**, *15*, 7472.
- [138] D. Walsh, J. D. Hopwood, S. Mann, *Science* **1994**, *264*, 1576.
- [139] K. K. Perkin, J. L. Turner, K. L. Wooley, S. Mann, *Nano Lett.* **2005**, *5*, 1457.
- [140] M. Breulmann, H. Cölfen, H.-P. Hentze, M. Antonietti, D. Walsh, S. Mann, *Adv. Mater.* **1998**, *10*, 237.
- [141] S.-H. Yu, H. Cölfen, *J. Mater. Chem.* **2004**, *14*, 2124.
- [142] H. Cölfen, S. Mann, *Angew. Chem.* **2003**, *115*, 2452; *Angew. Chem. Int. Ed.* **2003**, *42*, 2350.
- [143] A.-W. Xu, M. Yurong, H. Cölfen, *J. Mater. Chem.* **2007**, *17*, 415.
- [144] R. Tang, L. Wang, C. A. Orme, T. Bonstein, P. J. Bush, G. H. Nancollas, *Angew. Chem.* **2004**, *116*, 2751; *Angew. Chem. Int. Ed.* **2004**, *43*, 2697.
- [145] R. Montenegro, M. Antonietti, Y. Mastai, K. Landfester, *J. Phys. Chem. B* **2003**, *107*, 5088.
- [146] A. Taden, K. Landfester, *Macromolecules* **2003**, *36*, 4037.
- [147] R. Montenegro, K. Landfester, *Langmuir* **2003**, *19*, 5996.
- [148] M. Vennes, R. Zentel, M. Rossle, M. Stepputat, U. Kolb, *Adv. Mater.* **2005**, *17*, 2123.
- [149] S. O. Tongcher, R. Sigel, K. Landfester, *Langmuir* **2006**, *22*, 4504.
- [150] A. Taden, K. Landfester, M. Antonietti, *Langmuir* **2004**, *20*, 957.
- [151] M. Li, S. Mann, *Langmuir* **2000**, *16*, 7088.
- [152] A. Manzke, Ch. Phahler, O. Dubbers, A. Plettl, P. Ziemann, D. Crespy, E. Schreiber, U. Ziener, K. Landfester, *Adv. Mater.* **2007**, *19*, 1337.
- [153] S. Brieger, O. Dubbers, S. Fricker, A. Manzke, C. Pfahler, A. Plettl, P. Ziemann, *Nanotechnology* **2006**, *17*, 4991.
- [154] G. Kästle, H.-G. Boyen, F. Weigl, G. Lengel, T. Herzog, P. Ziemann, S. Riethmüller, O. Mayer, C. Hartmann, J. P. Spatz, M. Möller, M. Ozawa, F. Banhart, M. G. Garnier, P. Oelhafen, *Adv. Funct. Mater.* **2003**, *13*, 853.
- [155] A. Taden, M. Antonietti, A. Heilig, K. Landfester, *Chem. Mater.* **2004**, *16*, 5081.
-